

UC San Diego

UC San Diego Previously Published Works

Title

Investigation of Dipicolinic Acid Isosteres for the Inhibition of Metallo- β -Lactamases

Permalink

<https://escholarship.org/uc/item/0z35p59b>

Journal

ChemMedChem, 14(13)

ISSN

1860-7179

Authors

Chen, Allie Y
Thomas, Pei W
Cheng, Zishuo
et al.

Publication Date

2019-07-03

DOI

10.1002/cmdc.201900172

Peer reviewed



HHS Public Access

Author manuscript

ChemMedChem. Author manuscript; available in PMC 2020 July 03.

Published in final edited form as:

ChemMedChem. 2019 July 03; 14(13): 1271–1282. doi:10.1002/cmdc.201900172.

Investigation of Dipicolinic Acid Isosteres for the Inhibition of Metallo- β -Lactamases

Allie Y. Chen^[a], Pei W. Thomas^[b], Zishuo Cheng^[c], Nasa Y. Xu^[b], David L. Tierney^[c], Michael W. Crowder^[c], Walter Fast^[b], and Seth M. Cohen^[a]

^[a]Department of Chemistry and Biochemistry, University of California, San Diego, La Jolla, CA 92093, United States

^[b]Division of Chemical Biology & Medicinal Chemistry, College of Pharmacy University of Texas, Austin Austin, TX 78712, United States

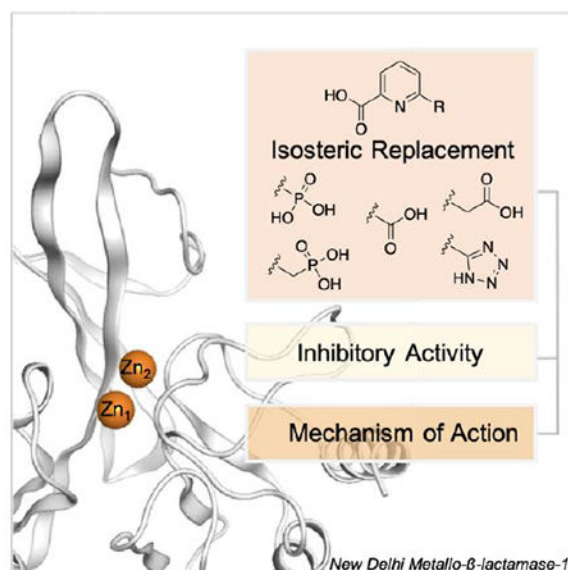
^[c]Department of Chemistry and Biochemistry, Miami University Oxford, OH 45056, United States

Abstract

New Delhi Metallo- β -lactamase-1 (NDM-1) poses an immediate threat to our most effective and widely prescribed drugs, the β -lactam containing class of antibiotics. There are no clinically relevant inhibitors to combat NDM-1, despite significant efforts towards their development. Inhibitors that utilize a carboxylic acid motif for binding the Zn(II) ions in the active site of NDM-1 comprise of a large portion of the >500 inhibitors reported to date. New and structurally diverse scaffolds for inhibitor development are of urgent need. Herein, we report the isosteric replacement of one carboxylate group of dipicolinic acid (**DPA**) to obtain **DPA** isosteres with good inhibitory activity against NDM-1 (and related metallo- β -lactamases, IMP-1 and VIM-2). It was determined that the choice of carboxylate isostere influences both the potency of NDM-1 inhibition and the mechanism of action. Additionally, we show that an isostere with a metal-stripping mechanism can be re-engineered into an inhibitor that favors ternary complex formation. This work provides a roadmap for future isosteric replacement of routinely used metal binding motifs (i.e., carboxylic acids) for the generation of new entities in NDM-1 inhibitor design and development.

Graphical abstract

Dipicolinic acid isosteres were evaluated against metallo- β -lactamases. The concept of isosteres is used to show the choice of the carboxylate isostere not only impacts inhibition value, but also the mechanism of action. This study demonstrates the utility of isosteric replacement for routinely used metal binding motifs (e.g., carboxylic acids) in metalloenzyme inhibitor development.



Keywords

Metal Binding Pharmacophores (MBP); Metallo- β -lactamase (MBL); New Delhi Metallo- β -lactamase (NDM-1); Verona Integrin-encoded Metallo- β -lactamase-2 (VIM-2); Imipenemase-1 (IMP-1); Dipicolinic acid (DPA); Isostere

Introduction

β -Lactam-containing antibiotics have been one of the most successful and popular class of antibiotics for combating a wide range of Gram-positive and -negative bacterial infections. Unsurprisingly, since the introduction of β -lactam containing antibiotics (beginning with penicillin in the 1940s), the widespread use of this class of antibiotics has led to the emergence of various resistance mechanisms. Resistance mechanisms that bacteria employ include mutation of penicillin binding proteins (PBPs), modification of outer membrane proteins, the production of efflux pumps, and the expression of β -lactamases.¹⁻² β -Lactamases utilize either an active site serine residue (Ambler classes A, C, and D) or Zn(II) metal ion(s) (Ambler class B, also known as metallo- β -lactamases, MBLs) to hydrolyze the β -lactam ring of the target antibiotic and render the drug ineffective.^{1, 3} A dedicated β -lactamase database provides an up-to-date compilation of the biochemical and structural data of all MBLs (<http://www.bldb.eu/>).⁴ First observed in 1966 by Sabath and Abraham (merely two decades after the introduction of penicillin), there are now >80 reported unique MBL families.^{3, 5} MBLs have become one of the most problematic bacterial resistance mechanisms due to their wide substrate profile, with the ability to hydrolyze virtually all clinically used bicyclic β -lactam antibiotics.⁶⁻⁷

MBLs are divided into B1, B2, and B3 subclasses depending on sequence identity and the number of Zn(II) ion(s) (either one or two) in the active site. Description of subclasses and their mechanism of action are reviewed elsewhere.⁶⁻⁹ Commonly observed and clinically relevant members of the MBLs belong to subclass B1,¹⁰ of which New Delhi Metallo- β -

lactamase (NDM) is a prominent representative. NDM bears a dinuclear Zn(II) active site, with Zn₁ ligated by H116, H118, H196, and a bridging hydroxide, and Zn₂ ligated by D120, C221, H263, the bridging hydroxide, and an apical H₂O (standard BBL numbering).¹¹ The active site is flanked between two flexible loops, allowing the protein to accommodate a wide range of antibiotic substrates.^{12–13} Plasmids that carry the *bla*_{NDM}-gene to undergo horizontal gene transfer between different species of microorganisms, leading to an increase in the prevalence of *bla*_{NDM}-bearing pathogens.^{14–15} Additionally, the threat of NDM is exacerbated (compared to the two other most prevalent members of the B1 MBLs, IMiPenemase, IMP, and Verona Integron-encoded Metallo-β-lactamase, VIM) by the ability of NDM to anchor to the cellular membrane, leading to higher protein stability and secretion.^{16–17} Resistance to a broad spectrum of β-lactams and the high horizontal gene transfer ability have allowed for rapid propagation from nosocomial infections to infections within the general population.^{18–20} Furthermore, *bla*_{NDM} is often carried on plasmids containing other genes that encode various resistance factors (including macrolides, aminoglycosides, rifampicin, and sulfamethoxazole),¹⁴ resulting in bacterial infections that are resistant to many different classes of antimicrobials.

It has been ten years since the first report of NDM-1, with >24 NDM variants currently identified.^{4, 14, 21} Some NDM variants exhibit an increase in thermal stability, Zn(II) affinity, and mononuclear Zn(II) activity that may provide an evolutionary advantage when Zn(II) availability is low.^{22–24} Unfortunately, even with the rapid spread of the *bla*_{NDM-1} gene and the evolution of NDM variants, little advancement has been made in inhibitor development. There are currently ~525 inhibitors reported in literature (representative structures shown in Figure 1),²⁵ but many inhibitors share similar structural features and none have progressed to clinical trials. The flexible active site of NDM-1, the diversity of related MBLs, a lack of understanding for inhibition mechanisms, and misinterpretation of structural data have all contributed to delayed inhibitor development.^{26–27} A survey of current NDM-1 inhibitors reveals a large portion of inhibitors bear a carboxylic acid motif.^{25–26} In line with this, our lab previously utilized a fragment-based drug discovery (FBDD) approach to identify dipicolinic acid (**DPA**) as a lead metal-binding pharmacophore (MBP) for NDM-1 inhibitor development.²⁸ Derivatization of **DPA** was performed to obtain 4-(3-aminophenyl)pyridine-2,6-dicarboxylic acid (Figure 1) as a highly selective inhibitor for NDM-1 (IMP-1 and VIM-2) that inhibits by forming a stable NDM-1:Zn(II):inhibitor ternary complex. In this study, we further investigate the **DPA** MBP as an inhibitor for NDM-1 utilizing the concept of isosteric replacement.

Isosteres bear similar structural and physical properties to the parent functional group and are used as surrogates in an effort improve the overall drug-likeness (i.e., increased permeability, better pharmacokinetics, and/or reduced toxicity) of the original molecule. A prominent example includes substituting the carboxylic acid functional group with carboxylic acid isosteres.^{37–38} There are an estimated >450 marketed drugs (including nonsteroidal anti-inflammatory drugs, antibiotics, anticoagulants, and cholesterol-lowering statins) that utilize a carboxylic acid motif.^{37–39} The ionizable nature of the carboxylic acid under physiological conditions (pH 7.4) makes it a useful handle for generating strong inhibitor-target interactions (i.e., electrostatic and hydrogen bonds). In metalloenzyme

inhibition, the carboxylic acid motif routinely participates in metal coordination, as seen in inhibitors for neutral endopeptidase (NEP), class II fructose-1,6-bisphosphate aldolase (FBP-aldolase), angiotensin-converting enzyme (ACE), and many others.⁴⁰ Despite the efficacy of this functional group, its usefulness can be limited in drug development due to poor cell permeability, metabolic instability, and off-target effects.^{37, 39} In an attempt to overcome such liabilities, chemists turn to the utilization of pro-drugs or isosteric replacement. Recent studies have begun to explore the effect of MBP isosteric replacement in metalloenzyme inhibition and pharmacokinetic profile.^{41–42}

In this study, we report the development and evaluation of 10 **DPA** isosteres (Figure 2) as inhibitors of NDM-1 and related MBLs. A selection of carboxylic acid isostere motifs was chosen to span a range of acidity (pK_a) values and metal coordination preferences. Varying the identity of the isostere impacts both inhibition value and inhibition mechanism. Additionally, we show the re-engineering of an isostere from a metal-stripping mechanism to one that favors the formation of a ternary complex. This study provides a roadmap for the isosteric replacement of current and future metal-binding motifs for the generation of new entities in NDM-1 inhibitor design and may be adopted for the inhibitor development of MBLs and other metalloenzymes.

Results and Discussion

Isostere Syntheses.

The synthesis of isosteres (**1** – **10**) is presented in Scheme 1, Scheme 2, and Scheme 3. Synthesis of isosteres **1**, **4**, **9**, and **10** are summarized in Scheme 1. Isostere **1** was obtained from a palladium-catalyzed Hirao cross-coupling reaction of commercially available methyl 6-bromopicolinate and diethylphosphate, followed by acid hydrolysis. Isostere **4** was achieved by conversion of the methyl 6-bromopicolinate to a nitrile via the Rosenmund-von Braun reaction, followed by an azide-nitrile cycloaddition. Isosteres **9** and **10** were synthesized via palladium-catalyzed Stille coupling of methyl 6-bromopicolinate with the corresponding organotin reagents, followed by saponification. Syntheses of isosteres **2**, **3**, **5**, **6**, and **8** are summarized in Scheme 2. Briefly, compound **11** was obtained from commercially available methyl 6-(hydroxymethyl)picolinate. Substitution of the alkyl bromide of compound **11** with various nucleophiles, followed by hydrolysis yielded isosteres **2**, **3**, **5**, **6**, and **8**. Lastly, methyl 6-aminopicolinate was treated with methanesulfonyl chloride, followed by saponification to yield isostere **7**.

Inhibition Assay.

A preliminary screen of isosteres **1** – **10** was performed against NDM-1 utilizing meropenem as substrate (at a single concentration of 180 μM , Table 1). Meropenem was observed to have a $K_{M,\text{NDM-1}} = 80 \pm 7 \mu\text{M}$ and $k_{\text{cat}} = 15.3 \pm 0.4 \text{ s}^{-1}$. Compounds **1** – **4** exhibited inhibition against NDM-1 with IC_{50} values ranging from 0.13 – 7.7 μM . Compounds **1** and **2** (both bearing a phosphonic acid) exhibited lower IC_{50} values (130 ± 10 and $310 \pm 10 \text{ nM}$, respectively) compared to that of **DPA** ($840 \pm 40 \text{ nM}$), while **3** and **4** revealed higher IC_{50} values (7.7 ± 0.6 and $7.0 \pm 0.5 \mu\text{M}$, respectively). Interestingly, compound **5**, which possesses a similar acidic motif as **1** and **2** (a sulfonic acid versus a phosphonic

acid) showed no inhibition at concentrations up to 10 μM . Notably, all compounds where the substituted moiety was not acidic (**6** – **10**) showed no appreciable inhibition at concentrations up to 10 μM .

To determine the ability of isosteres to inhibit other B1 MBLs, the inhibition of **1** – **4** against NDM-1, IMP-1, and VIM-2 was investigated. An alternative substrate, Fluorocillin ($K_{\text{M, NDM-1}} = 460 \text{ nM}$), was utilized to increase assay sensitivity.^{28, 43} Lower IC_{50} values for Fluorocillin compared to meropenem were expected due to using a smaller $[\text{S}]/K_{\text{M}}$ ratio in these experiments. IC_{50} values determined for NDM-1 inhibition via Fluorocillin showed the same trends as with meropenem, with **1** and **2** showing the lowest IC_{50} values, followed by the parent **DPA** fragment, with **3** and **4** yielding higher IC_{50} values among these five compounds (Table 2). Similar trends, but with IC_{50} values about an order of magnitude higher, were observed for IMP-1 (Table S1, Figure S1) and VIM-2 as well.

Equilibrium Dialysis.

Equilibrium dialysis experiments were performed to give insight into the inhibition mechanism (metal stripping versus ternary complex formation) of **DPA** and the active isosteres. After protein purification, NDM-1 was exchanged into ammonium acetate buffer to facilitate the use of ICP-AES in determining metal content. Metal analyses of the resulting protein showed that the enzyme binds ~ 1.7 equivalents of Zn(II) (Figure 3). While holoNDM-1 is expected to bind 2 equivalents of Zn(II), previous studies have shown that one of the Zn(II) ions binds more weakly than the other, resulting in protein that contain less than the full complement of two Zn(II) ions.^{44–45} As previously reported, incubation of NDM-1 with L-captopril, a known competitive inhibitor (Figure 1),⁴⁶ did not show any evidence of Zn(II) removal. In contrast, the Zn(II) content of NDM-1 was significantly reduced when incubated with **DPA**.²⁸ Isosteres **1** – **4** exhibited different levels of Zn(II) removal from NDM-1. Compounds **3** and **4** behaved more like captopril, removing only small amounts of Zn(II) from NDM-1 even at concentrations up to 128 μM . Conversely, compounds **1** and **2** removed more Zn(II) from NDM-1 than the parent **DPA**.

UV–Visible Spectroscopy.

As previously reported, UV-vis spectrophotometry of Co(II)-substituted NDM-1 can be used to probe inhibitor binding to the enzyme.²⁸ The spectrum of CoCo-NDM-1 shows an intense peak between 320 – 350 nm, which has been assigned to a cysteine-to-Co(II) ligand-to-metal charge transfer (LMCT) band, and multiple peaks between 500 – 650 nm, which have been assigned to Co(II) ligand field bands (Figure 4).^{22, 47} The inclusion of captopril to the sample results in large changes in the ligand field transitions, and an increase in the LMCT band. These changes are consistent with the formation of a NDM-1:captopril ternary complex, with the captopril sulfur bridging the two Co(II) ions.⁴⁸ Incubation of CoCo-NDM-1 with EDTA resulted in significant reduction of the LMCT and ligand field peaks, indicating that EDTA strips the metal from NDM-1.²⁸ Incubation of CoCo-NDM-1 with compounds **1** – **4** and **DPA** resulted in a reduction of absorbance at 500 – 650 nm (Figure 4), which indicates that Co(II) is being removed from the active site to varying degrees. Compound **2** appears to remove the most Co(II), followed by compound **1**, **DPA**, **3**, and then

4. The findings with CoCo-NDM-1 are wholly consistent with the equilibrium dialysis results.

Derivatization of Isostere 2.

Although **2** was shown to remove Zn(II) from NDM-1, we sought to reduce the metal-removal behavior via elaboration using a fragment-growth strategy. We previously had success using this approach to optimize **DPA**.²⁸ Also during the time of this study, a structure of **2** in complex with IMP-1 (PDB 5HH4) was reported.⁴⁹ In this structure, the Zn₁ of IMP-1 is coordinated via residues H116, H118, H196, and a bridging hydroxide in a tetrahedral coordination geometry (Figure 5, standard BBL numbering). The bridging hydroxide also coordinates to Zn₂, which is further ligated by residues D120, C221, and H263, as well as by the pyridine nitrogen donor and carboxylic acid of **2** (in an overall octahedral coordination geometry). The phosphonic acid motif of **2** is shown to hydrogen bond with the bridging hydroxide ion and a nearby S80 residue. Guided by this crystallographic data and the homology of IMP-1 and NDM-1 enzymes, a small library of **2** derivatives (**18a** – **18m**) were designed, synthesized, and tested for NDM-1 inhibition.

The synthesis of **18a** – **18m** is presented in Scheme 4 and the IC₅₀ values (measured for NDM-1 catalyzed hydrolysis of meropenem) are reported in Table 3. This library consisted of simple aryl derivatives substituted at the 4-position of the pyridine ring. The aryl ring bears substituents (methoxy, hydroxyl, amine, and chlorine) in the *para*-, *ortho*-, and *meta*-position of the ring in attempt to generate interactions with nearby residue side chains. To prepare these compounds, 4-hydroxypyridine-2,6-dicarboxylic acid was esterified to **12** with MeOH and catalytic H₂SO₄. Next, **12** was converted to **13** with tetrabutylammonium bromide (TBAB) and phosphorus pentoxide (P₄O₁₀). Compound **13** was treated with sodium borohydride (NaBH₄) at 0 °C to obtain **14**, which was further converted to intermediate **15** via phosphorous tribromide (PBr₃). Compound **16** was obtained by heating **15** and triethyl phosphite in toluene at 140 °C for 22h. Intermediates **17a** – **17m** were obtained via Suzuki cross-coupling procedures utilizing the corresponding boronic acid, (Pd(PPh₃)₄), and K₃PO₄. Compounds **18a** – **18m** were obtained via hydrolysis.

Compounds **18a** – **18m** did not yield greater inhibitory activity than that of **2** (IC₅₀ = 0.13±0.01 μM). A simple aryl ring (**18a**), or an aryl ring with methoxy (**18b** – **18d**) or hydroxyl substituent (**18e** – **18g**) were generally well-tolerated, with IC₅₀ = 0.20±0.01 – 0.48±0.01 μM, but did not lead to a marked decrease IC₅₀ value compared to that of **2**. Given the structural similarity of **18h** – **18j** (bearing the aniline substituent) to the previous reported inhibitor, (4-(3-aminophenyl)pyridine-2,6-dicarboxylic acid) (Figure 1), no improvement in inhibition was observed compared to that of **2** (IC₅₀ = 0.24±0.01 – 0.40±0.02 μM). Notably, a chlorine substituent in the *ortho*- and *meta*- position of the aryl ring yield a 2- to 3-fold loss in potency. Due to the similarities between the observed inhibition values, no structure-activity relationship (SAR) could be obtained. Although isosteric replacement of the carboxylate group maintains the ability to bind metal ions, the relative positioning of attached substituents is likely altered, possibly due to changes in metal coordination geometries. In the case of **DPA** and NDM-1, this prevents a simple

group-swapping approach, and may necessitate re-optimization starting with the new isostere fragment.

Although lower IC_{50} values for compounds **18a** – **18m** (compared to that of isostere **2**) were not observed, previous evaluation of DPA isosteres **1** – **4** has shown that an increase in IC_{50} value may be due to a shift in inhibitor mechanism (from metal stripping to ternary complex formation). To evaluate if this was the case for **18a** – **18m**, two candidates (**18b** and **18i**) were selected for further inhibition mechanism analysis. Indeed, dialysis experiment revealed **18b** and **18i** did not perturb the Zn(II) content of NDM-1 at concentrations as high as 16 μ M, with only slight Zn(II) removal at concentration of 32 μ M (Figure S2). In addition, one equivalent of Zn(II) was retained at the highest tested concentration (128 μ M) for **18b** and **18i**, while less than one equivalent was retained when performing the same experiment with compound **2**. This further supports our previous findings and shows the possibility to re-engineer a compound which removes metal from the active site of NDM-1 to one which favors ternary complex formation.

Herein, we investigate the isosteric replacement of a carboxylic acid group of **DPA** with various surrogate structures. Compounds **1** – **10** yield a range of chemical diversity (various acidic or metal-binding groups) and show that the choice of the carboxylate isostere not only impacts the IC_{50} value, but also the propensity for metal removal. Replacement of one carboxylic acid with a phosphonic substituent (**2**) results in a MBP with an extraordinarily low IC_{50} value, but also with a greater tendency for NDM-1 Zn(II) removal. Replacement of the carboxylic acid with a tetrazole motif (**4**) yield a higher IC_{50} value, but reduces NDM-1 Zn(II) removal. Equilibrium dialysis data, in conjunction with UV-vis spectroscopy of CoCoNDM-1, reveals differences in inhibition mechanism: inhibition by **2** occurs primarily via Zn(II) removal, likely forming the inactive mono-Zn(II) NDM-1, while inhibition by **4** is mainly via formation of a ternary complex at the dinuclear Zn(II) site. Because **4** forms a ternary complex at the active site, we can use IC_{50} and the Cheng-Prusoff relationship for competitive inhibitors to calculate a K_i of $2.2 \pm 0.5 \mu$ M.⁵⁰ It is important to note that calculating K_i values for metal-stripping inhibitors (such as **1** or **2**) is not appropriate because changes in IC_{50} may not reflect changes in binding affinity. Available data suggesting potential varying inhibition mechanisms between homologous MBLs and **2** (ternary complex formation with IMP-1,⁴⁹ but metal-stripping with NDM-1) was unexpected. This difference may be due to a lower binding affinity for Zn(II) in the Zn₂ site of NDM-1 ($K_d = 2 \mu$ M)⁴⁵ compared to that of IMP-1 ($K_d = 0.3 \mu$ M),^{51–52} resulting in more facile metal removal. Future studies are required to elucidate and conclude the observed mechanistic differences of **2** against IMP-1 and NDM-1.

In an attempt to reduce the propensity to strip metal from the NDM-1 active site, a small library of derivatives of compound **2** were synthesized (compounds **18a** – **18m**). It was predicted that **18i**, bearing the same amine backbone as a reported inhibitor that uses **DPA** as a metal-binding group, would result in a decrease in the observed IC_{50} value. Unfortunately, **18i** (and other derivatives) did not yield a lower IC_{50} value than that of **2**, suggesting that the isosteres are not exactly equivalent substitutions of their parent fragment. Isosteric replacement may alter the relative positioning of distant substituents and would necessitate further optimization. Additionally, compounds **18a** – **18m** were screened against IMP-1

(Supporting Information); however, no structure activity relationship was observed, with relatively flat IC_{50} values spanning $1.20 \pm 0.05 - 4.1 \pm 0.2 \mu M$. Dialysis experiment of derivatives **18b** and **18i** against NDM-1 reveal a reduced tendency to remove Zn(II) from the NDM-1 active site, albeit no reduction in the IC_{50} value, compared to that of isostere **2** (Figure S2).

Despite the understanding that compounds can inhibit MBLs via a number different mechanisms (covalent inhibition, metal-chelation, reversible competitive inhibition, allosteric inhibition, etc.), the mechanism of action of most reported MBL inhibitors is not well defined.²⁶ Many current studies focus on achieving low IC_{50} values, with little consideration regarding the mechanism of action. Here, we clearly demonstrate how the mechanism of inhibition can significantly differ between similar isosteres and homologous enzymes and illustrate challenges to optimizing inhibitors with metal-stripping mechanisms. In the design of future MBL inhibitors, a loss of potency may be preferred when selecting compounds with a desired mechanism of action for further optimization (i.e., selection of **4** over **2**). This kind of early stage evaluation of how the inhibitor interacts with the active site will be crucial for accelerating NDM (and other MBLs) inhibitor development.

Conclusions

In summary, we report the synthesis and inhibitory activity of ten **DPA** isosteres and investigated the mechanism of action of the most active compounds. We show that the exchange of the carboxylic acid with other acidic isosteres not only drastically affects the IC_{50} value but also the mechanism of action. The compounds which showed double-digit nanomolar IC_{50} is predicted to act via a metal-stripping mechanism, while compounds which displayed single-digit micromolar IC_{50} is predicted to form a ternary complex with the enzyme. Preliminary data suggests differences in inhibition mechanism between homologous NDM-1 and IMP-1 and isostere **2**. Additionally, we demonstrate the potential to morph metal-stripping compounds into inhibitors which favor ternary complex formation. This study demonstrates the importance of considering the inhibition mechanism, and the utility of bioisosteric replacement for routinely-used metal binding motifs (i.e., carboxylic acid) in NDM-1 inhibitor development.

Experimental Section

All reagents and solvents were obtained from commercial sources and used without further purification. Corning UV-transparent 96-well microplates (3635), Corning black polystyrene round-bottom 96-well microplates (3792), 3-((3-cholamidopropyl)-dimethylammonio)-1-propanesulfonate (CHAPS), 4-(2-hydroxyethyl)-1-piperazineethanesulfonic acid (HEPES), dimethyl sulfoxide (DMSO), L-captopril and Fluorocillin green 495/525 β -lactamase substrate, soluble product, were purchased from Thermo Fisher Scientific Inc. (Fair Lawn, NJ). All other reagents were purchased from Sigma-Aldrich Inc. (St. Louis, MO). Screening assays were performed on a PerkinElmer Victor3 V 1420 multilabel counter plate reader. Fluorescent assays were performed on a PerkinElmer Victor3 V fluorescent plate reader. Column chromatography was performed using a Teledyne ISCO CombiFlash Rf system with prepacked silica cartridges. All 1H NMR and ^{13}C spectra were recorded at either

ambient temperature or at 35 °C using Varian 400 Mercury Plus or Varian VX500 instrument located in the Department of Chemistry and Biochemistry at the University of California, San Diego. Mass spectrometry data were obtained from the University of California San Diego Chemistry and Biochemistry Mass Spectrometry Facility (MMSF). The purity of all compounds used for screening were determined to be 95% by high performance liquid chromatography (HPLC).

6-Phosphonopicolinic acid (1).

A solution of methyl 6-bromopicolinate (300 mg, 1.39 mmol), diethylphosphate (172.0 μ L, 1.39 mmol), Pd₂(dba)₃ (67 mg, 0.69 mmol), Pd(dppf)Cl₂ (77 mg, 0.14 mmol), and trimethylamine (387.0 μ L, 2.78 mmol) were dissolved in toluene (10 mL), and heated to 90°C for 20 h. Ethyl acetate (20 mL) was added to the reaction mixture, and the solution was filtered through a pad of celite. The collected organic layers were concentrated *in vacuo*. The crude mixture was purified via flash column chromatography, with the intermediate eluting at 50% ethyl acetate in hexanes. The intermediate was heated under reflux conditions with 6 M HCl (3 mL) for 20 h. The excess HCl was removed *in vacuo*, and co-evaporated with copious amounts of methanol and water until a precipitate was observed. The product was collected via vacuum filtration as a white solid in 19% yield (54 mg, 0.27 mmol). ¹H NMR (400 MHz, MeOD-*d*₄): δ = 8.26 (d, *J* = 7.7 Hz, 1H), 8.19 – 8.00 (m, 2H). ¹³C NMR (126 MHz, DMSO-*d*₆): δ 166.4, 156.2, 149.0, 138.0, 129.4, 126.1. ESI-MS(–) calculated for [C₆H₅NO₅P][–] *m/z* 202.10, found *m/z* 201.98 [M-H][–].

6-(Phosphonomethyl)picolinic acid (2).

A solution of **11** (200 mg, 0.87 mmol) and P(OEt)₃ (1.6 g, 9.56 mmol) were heated in toluene (20 mL) at 140°C for 2 h to give a clear liquid solution. Excess P(OEt)₃ and toluene were removed *in vacuo*, and the intermediate was purified via flash column chromatography eluting at 100% ethyl acetate in hexanes as a clear oil in 80% yield (200 mg, 0.70 mmol). ¹H NMR (400 MHz, CDCl₃-*d*): δ 8.02 (d, *J* = 8.0 Hz, 1H), 7.80 (td, *J* = 7.8, 2.1 Hz, 1H), 7.62 (d, *J* = 8.0 Hz, 1H), 4.13 – 4.06 (m, 4H), 3.99 (d, *J* = 2.0 Hz, 3H), 3.53 (d, *J* = 22.0 Hz, 2H), 1.31 – 1.25 (m, 6H). ESI-MS(+) calculated for [C₁₂H₁₉NO₅P]⁺ *m/z* 288.10, found *m/z* 288.29 [M+H]⁺.

The intermediate, methyl 6-((diethoxyphosphoryl)methyl)picolinate (200 mg, 0.70 mmol) was refluxed in 6 M HCl (5 mL) for 27 h. The excess HCl was removed *in vacuo* and co-evaporate with copious amounts of methanol and water until a white precipitate was observed. Compound **2** was collected via vacuum filtration as a white solid in 86% yield (130 mg, 0.60 mmol). ¹H NMR (400 MHz, DMSO-*d*₆): δ 8.02 (t, *J* = 7.7 Hz, 1H), 7.95 (d, *J* = 7.5 Hz, 1H), 7.67 (d, *J* = 7.6 Hz, 1H), 3.38 (s, 1H), 3.32 (s, 1H). ¹³C NMR (126 MHz, DMSO-*d*₆): δ 166.6, 155.4, 148.0, 137.9, 127.8, 122.8, 38.3. ESI-MS(–) calculated for [C₇H₈NO₅P][–] *m/z* 217.01, found *m/z* 216.00 [M-H][–].

6-(Carboxymethyl)picolinic acid (3).

To a solution of **11** (2.5 g, 10.87 mmol) dissolved in THF (50 mL) was added a pre-dissolved solution of KCN (1.1 g, 16.30 mmol) in water (9 mL). All supplies in contact with KCN were quenched with 1 M sodium thiosulfate prior to disposal. The mixture was stirred

at 50 °C for 19 h and quenched with 1 M sodium thiosulfate solution. The mixture was extracted with CH₂Cl₂ (25 mL X5). The combined organic layers were dried over MgSO₄, filtered, and concentrated *in vacuo*. Intermediate methyl 6-(cyanomethyl)picolinate was purified via flash column chromatography, eluting at 58% ethyl acetate in hexanes to yield yellow crystals in 49% yield (941 mg, 5.34 mmol). ¹H NMR (400 MHz, DMSO-*d*₆): δ 8.09 – 7.95 (m, 2H), 7.68 (t, *J* = 5.5 Hz, 1H), 4.30 (s, 2H), 3.88 (s, 3H). ESI-MS(+) calculated for [C₉H₉N₂O₂]⁺ *m/z* 177.06, found *m/z* 177.18 [M+H]⁺.

The intermediate, methyl 6-(cyanomethyl)picolinate was dissolved in 12 M HCl and heated to 100 °C for 12 h. The solvent was removed *in vacuo* and the crude was hydrolyzed in 3 mL of 1 M NaOH at 60 °C for 6 h. The solution was acidified with 4 M HCl to pH 4, and product **3** was collected via vacuum filtration as a white solid in 30% yield (37 mg, 0.20 mmol). ¹H NMR (400 MHz, DMSO-*d*₆): δ 7.98 – 7.86 (m, 2H), 7.56 (d, *J* = 6.3 Hz, 1H), 3.83 (s, 2H). ¹³C NMR (126 MHz, DMSO-*d*₆): δ 172.1, 166.6, 155.8, 148.3, 138.3, 128.0, 123.4, 43.6. ESI-MS(+) calculated for [C₈H₈NO₄]⁺ *m/z* 182.04, found *m/z* 182.25 [M+H]⁺.

6-(1H-Tetrazol-5-yl)picolinic acid (**4**).

Methyl 6-bromopicolinate (3 g, 13.886 mmol) and copper(I) cyanide (2.49 g, 27.77 mmol) were dissolved in pyridine (120 mL) and heated to 116 °C for 4 h. The reaction was monitored via TLC. Upon completion of the reaction, the mixture was filtered, and the filtrate was concentrated *in vacuo*. Aqueous NaHCO₃ (50 mL) and CH₂Cl₂ (50 mL) were added to the crude mixture. The aqueous layer was extracted with CH₂Cl₂ (50 mL X 3), and the combined organic layers were dried over MgSO₄, concentrated *in vacuo*, and purified with flash chromatography. Intermediate methyl 6-cyanopicolinate eluted 40% ethyl acetate in hexanes as a yellow solid in 20% yield (470 mg, 2.90 mmol). ¹H NMR (400 MHz, CDCl₃-*d*): δ 8.34 (d, *J* = 7.9 Hz, 1H), 8.04 (t, *J* = 7.9 Hz, 1H), 7.88 (d, *J* = 7.8 Hz, 1H), 4.04 (s, 3H). ESI-MS(+) calculated for [C₈H₇N₂O₂]⁺ *m/z* 163.05, found *m/z* 163.10 [M+H]⁺.

In a round bottom flask, intermediate methyl 6-cyanopicolinate (200 mg, 1.23 mmol), sodium azide (408 mg, 6.29 mmol), and ammonia hydrochloride (336 mg, 6.29 mmol) were dissolved in anhydrous DMF (10 mL). The reaction was heated under N₂ at 130 °C for 20 h. After cooling, the inorganic salts were removed via vacuum filtration, and washed with hot DMF. The organic filtrate was concentrated *in vacuo* to yield a yellow solid. The solid was suspended in a solution of 2 M HCl (3 mL), and stirred at 25 °C for 1 h. The precipitate was collected via vacuum filtration and washed with copious amounts of cold water to afford product **4** as a white solid in 98% yield (232 mg, 1.21 mmol). ¹H NMR (400 MHz, DMSO-*d*₆): δ 8.37 (d, *J* = 7.5 Hz, 1H), 8.26 – 8.13 (m, 2H). ¹³C NMR (126 MHz, DMSO-*d*₆): δ 165.2, 155.1, 149.1, 144.3, 140.3, 126.8, 126.2. ESI-MS(–) calculated for [C₇H₄N₅O₂][–] *m/z* 190.04, found *m/z* 189.25 [M-H][–].

6-(Sulfomethyl)picolinic acid (**5**).

In a round bottom flask, **11** (200 mg, 0.87 mmol) and Na₂SO₃ (110 mg, 0.87 mmol) were dissolved in H₂O (10 mL), and heated to 100 °C for 16 h. The reaction was cooled to room temperature, and H₂O was removed *in vacuo* until it reached one-third of the original volume. The white precipitate was collected via vacuum filtration as the ester intermediate.

The intermediate was hydrolyzed via stirring in 4 M HCl at 100 °C for 16 h. The excess HCl was removed *in vacuo*, and the product was co-evaporated with copious amounts of MeOH and H₂O until white crystals were observed. The precipitate was collected via vacuum filtration to yield compound **5** as a white crystal in 41% yield (77.0 mg, 0.35 mmol). ¹H NMR (400 MHz, DMSO-*d*₆): δ 8.08 – 7.88 (m, 2H), 7.79 (d, *J* = 6.0 Hz, 1H), 4.06 (s, 2H). ¹³C NMR (126 MHz, DMSO-*d*₆): δ 164.7, 155.0, 145.2, 140.7, 129.9, 124.1, 57.6. ESI-MS(–) calculated for [C₇H₆NO₅S][–] *m/z* 216.10, found *m/z* 216.08 [M-H][–].

6-((Methylsulfonyl)methyl)picolinic acid (**6**).

In a round bottom flask, **11** (300 mg, 1.30 mmol) and sodium methanesulfinate (266 mg, 2.61 mmol) were dissolved in DMF (15 mL). The solution was heated to 120 °C for 2 h. DMF was removed *in vacuo*, and the crude product was purified via flash column chromatography eluting at 90% ethyl acetate in hexanes. The intermediate was hydrolyzed by stirring in 3:1 1M NaOH:THF at 70 °C for 3 h. The THF was removed *in vacuo*, and the solution was acidified with 4 M HCl until pH 4. The aqueous layer was extracted with ethyl acetate (20 mL X 3) to afford **6** a white solid in 43% yield over two steps (120 mg, 0.56 mmol). ¹H NMR (400 MHz, DMSO-*d*₆): δ 8.03 (s, 2H), 7.70 (t, *J* = 4.5 Hz, 1H), 4.75 (s, 2H), 3.08 (s, 3H). ¹³C NMR (126 MHz, DMSO-*d*₆): δ 166.3, 150.7, 149.2, 138.9, 129.3, 124.5, 61.5, 41.1. ESI-MS(–) calculated for [C₈H₈NO₄S][–] *m/z* 214.02, found *m/z* 214.16 [M-H][–].

6-(Methylsulfonamido)picolinic acid (**7**).

Commercially available methyl 6-aminopicolinate (300 mg, 1.97 mmol) was dissolved in a solution of triethylamine (1 mL):CH₂Cl₂ (5 mL) and cooled to 0 °C. Next, methanesulfonyl chloride (168.0 μL, 2.17 mmol) was added drop-wise to the mixture. The reaction was stirred at room temperature for 16 h. The solvent was removed *in vacuo*, and the crude mixture was purified via flash column chromatography. The ester intermediate eluted at 62% ethyl acetate in hexanes as a white solid. The intermediate was hydrolyzed via stirring at room temperature for 16 h in 3:1 1M NaOH:THF (8 mL). The excess THF was removed *in vacuo*, and the solution was acidified with 4 M HCl to pH 4. The aqueous layer was extracted with ethyl acetate (10 mL X 3), and the combined organic layers were dried over MgSO₄, filtered, and concentrated *in vacuo* to afford **7** as a white solid. ¹H NMR (400 MHz, MeOD-*d*₄): δ 7.89 (t, *J* = 7.9 Hz, 1H), 7.79 (d, *J* = 7.5 Hz, 1H), 7.28 (d, *J* = 8.3 Hz, 1H), 3.33 (s, 3H). ¹³C NMR (126 MHz, DMSO-*d*₆): δ 166.2, 152.4, 147.1, 140.1, 119.5, 115.9, 42.5. ESI-MS(–) calculated for [C₇H₇N₂O₄S][–] *m/z* 215.10, found *m/z* 215.05 [M-H][–].

6-((N-Methylmethylsulfonamido)methyl)picolinic acid (**8**).

In a round bottom flask, **11** (158 mg, 0.69 mmol), *N*-methylmethanesulfonamide (74 mg, 0.69 mmol), and potassium carbonate (48 mg, 0.34 mmol) were dissolved in acetonitrile (10 mL) and heated to 75 °C for 20 h. The solvent was removed *in vacuo* and the crude mixture was purified via flash column chromatography. The ester intermediate eluted at 3% MeOH in CH₂Cl₂ as a yellow oil. The intermediate was hydrolyzed by stirring in 1 M NaOH at 70 °C for 3 h. The solution was acidified with 4 M HCl to pH 4, and the aqueous layer was extracted with ethyl acetate (20 mL X 4). The combined organic layers were dried over

MgSO₄, filtered, and concentrated in vacuo to afford **8** a pale solid in 55% yield over two steps (92 mg, 0.38 mmol). ¹H NMR (400 MHz, DMSO-*d*₆): δ 8.04 – 7.90 (m, 2H), 7.61 (d, *J* = 7.3 Hz, 1H), 4.46 (s, 2H), 3.08 (s, 3H), 2.75 (s, 3H). ¹³C NMR (126 MHz, DMSO-*d*₆): δ 166.5, 157.4, 148.5, 138.9, 125.7, 124.1, 54.9, 36.7, 35.2. ESI-MS(–) calculated for [C₉H₁₁N₂O₄S][–] *m/z* 243.04, found *m/z* 243.31 [M-H][–].

6-(Thiazol-2-yl)picolinic acid (**9**).

In a round bottom flask, methyl 6-bromopicolinate (300 mg, 1.39 mmol) and 2-(tributylstannyl)thiazole (624 mg, 1.67 mmol) were dissolved in anhydrous THF (15 mL). The solution was purged with N₂ for 15 min, followed by the addition of bis(triphenylphosphine)palladium(II) dichloride (97 mg, 0.14 mmol). The reaction was heated to 75°C for 18 h. Upon completion, water (20 mL) and ethyl acetate (20 mL) were added to the brown slurry. The aqueous layer was extracted with ethyl acetate (20 mL X 3), and the combined organic layers were dried over MgSO₄, filtered, and concentrated in vacuo. The ester intermediate was purified via column chromatography, eluting at 45% ethyl acetate in hexanes as a yellow solid. The intermediate was hydrolyzed in 3:1 1 M NaOH:THF at 70 °C for 3 h. THF was removed in vacuo, and the aqueous layer was acidified with 4 M HCl to pH 4. The precipitate was collected via vacuum filtration to afford compound **9** as a tan solid in 74% yield (213 mg, 1.03 mmol). ¹H NMR (400 MHz, DMSO-*d*₆): δ 9.18 (s, 1H), 8.68 (s, 1H), 8.22 (d, *J* = 8.0 Hz, 1H), 8.05 (t, *J* = 7.8 Hz, 1H), 7.94 (d, *J* = 7.7 Hz, 1H). ¹³C NMR (126 MHz, DMSO-*d*₆): δ 166.1, 157.0, 150.5, 149.0, 142.3, 139.7, 139.1, 124.2, 123.4. ESI-MS(–) calculated for [C₉H₅N₂O₂S][–] *m/z* 205.01, found *m/z* 205.18 [M-H][–].

6-(Oxazol-2-yl)picolinic acid (**10**).

In a round bottom flask, methyl 6-bromopicolinate (300 mg, 1.39 mmol) and 2-(tributylstannyl)oxazole (596 mg, 1.67 mmol) were dissolved in anhydrous THF (15 mL). The solution was purged with N₂ for 15 min, followed by the addition of bis(triphenylphosphine)palladium(II) dichloride (79 mg, 0.14 mmol). The solution was heated to 75°C for 18 h. Upon completion, water (20 mL) and ethyl acetate (20 mL) were added to the slurry. The aqueous layer was extracted with ethyl acetate (20 mL X 3), and the combined organic layers were dried over MgSO₄, filtered, and concentrated in vacuo. The ester intermediate was purified via column chromatography, eluting at 60% ethyl acetate in hexanes as a yellow solid. The intermediate was hydrolyzed in 3:1 1 M NaOH:THF at 70°C for 3 h. THF was removed in vacuo, and the aqueous layer was acidified with 4 M HCl until pH 4. The aqueous layer was extracted with ethyl acetate (20 mL X 3), and the combined organic layers were dried over MgSO₄, filtered, and concentrated in vacuo to yield **10** as a white solid in 8% yield (20 mg, 0.12 mmol). ¹H NMR (400 MHz, DMSO-*d*₆): δ 8.35 (s, 1H), 8.28 (dd, *J* = 6.4, 2.6 Hz, 1H), 8.16 – 8.10 (m, 2H), 7.49 (s, 1H). ¹³C NMR (126 MHz, DMSO-*d*₆): δ 166.2, 160.0, 149.4, 145.9, 142.0, 139.4, 129.4, 126.2, 125.3. ESI-MS(–) calculated for [C₉H₅N₂O₃][–] *m/z* 189.03, found *m/z* 189.20 [M-H][–].

Methyl 6-(bromomethyl)picolinate (11).

To a solution of methyl 6-(hydroxymethyl)picolinate (1.0 g, 5.98 mmol) in chloroform (25 mL) at 0°C was added PBr₃ (1.9 g, 7.18 mmol) dropwise over the course of 15 min. The reaction was stirred at room temperature for 3 h. The reaction mixture was quenched with saturated sodium carbonate in water and extracted with chloroform (20 mL X 4). The combined organic layers were dried over MgSO₄, filtered, and concentrated in vacuo. The product was purified via flash column chromatography, eluting at 45% ethyl acetate in hexanes to afford **11** as a white crystal in 70% yield (95 mg, 4.14 mmol). ¹H NMR (400 MHz, CDCl₃-*d*): δ 8.06 (d, *J* = 7.8 Hz, 1 H), 7.86 (td, *J* = 7.8, 1.4 Hz), 7.68 (d, *J* = 7.8 Hz, 1 H), 4.64 (s, 2H), 4.01 (s, 3H). ESI-MS(+) calculated for [C₈H₉BrNO₂]⁺ *m/z* 229.98, found *m/z* 230.24 [M+H]⁺.

Dimethyl 4-hydroxypyridine-2,6-dicarboxylate (12).

Commercially-available 4-hydroxypyridine-2,6-dicarboxylic acid (10.0 g, 55 mmol) was dissolved in MeOH (500 mL) and H₂SO₄ (cat.) was added. The reaction was stirred at 70°C for 16 h. The solvent was removed in vacuo, and the crude mixture was purified via column chromatography, eluting at 1% MeOH in CH₂Cl₂ as a yellow solid in 60% yield (7.0 g, 30 mmol). ¹H NMR (400 MHz, MeOD-*d*₄): δ 7.59 (s, 2H), 3.96 (s, 6H). ESI-MS(+) calculated for [C₉H₁₀NO₅]⁺ *m/z* 212.06, found *m/z* 212.07 [M+H]⁺.

Dimethyl 4-bromopyridine-2,6-dicarboxylate (13).

Tetrabutylammonium bromide (28.623 g, 88.789 mmol) and phosphorus(V) oxide (12.6 g, 89 mmol) were dissolved in dry toluene (50 mL), and heated to 100°C for 30 min under N₂. Compound **12** (7.5 g, 36 mmol) was added to the solution and the mixture was heated at 100 °C for 3 h. The toluene layer was decanted, and an additional 50 mL of toluene was added to the residual brown oil. The mixture was heated to 100°C for an additional 30 min, and the toluene layer was decanted again. Addition and removal of toluene was repeated three times. The combined toluene layers were dried in vacuo, and the crude mixture was purified via column chromatography. Compound **13** eluted at 45% ethyl acetate in hexanes as yellow needles in 75% yield (7.3 g, 27 mmol). ¹H NMR (400 MHz, DMSO-*d*₆): δ 8.42 (s, 2H), 3.91 (s, 6H). ESI-MS(+) calculated for [C₉H₉BrNO₄]⁺ *m/z* 273.97, found *m/z* 274.26 and 275.25 [M+H]⁺.

Methyl 4-bromo-6-(hydroxymethyl)picolinate (14).

In a round bottom flask, compound **13** (1.0 g, 3.65 mmol) was dissolved in a solution of MeOH:CH₂Cl₂ (16 mL:4 mL) and cooled to 0°C. NaBH₄ (138 mg, 3.65 mmol) was added to the mixture and stirred at 0°C for 1 h. The reaction was quenched with aqueous NaHCO₃ (10 mL). The mixture was extracted with CH₂Cl₂ (10 mL X 3), and the combined organic layers were dried in vacuo. The crude mixture was purified via column chromatography, with **14** eluting at 70% ethyl acetate in hexanes as a white crystal in 80% yield (689 mg, 2.80 mmol). ¹H NMR (400 MHz, MeOD-*d*₄): δ 8.17 (s, 1H), 7.97 (s, 1H), 4.73 (s, 2H), 3.97 (s, 3H). ESI-MS(+) calculated for [C₈H₉BrNO₃]⁺ *m/z* 245.98, found *m/z* 246.16 and 248.09 [M+H]⁺.

Methyl 4-bromo-6-(bromomethyl)picolinate (15).

Compound **14** (400 mg, 1.63 mmol) was dissolved in CHCl_3 (4 mL) and cooled to 0°C . Next, PBr_3 (528 mg, 1.95 mmol) was added dropwise, and the reaction was stirred at 0°C for 1 h. The reaction was tracked via TLC. Upon completion, the reaction mixture was quenched with aqueous Na_2CO_3 (40 mL), and the aqueous layer was extracted with chloroform (40 mL X 4). The combined organic layers were dried over MgSO_4 , filtered, and concentrated in vacuo to yield a yellow oil with white precipitate. The crude product was purified via flash column chromatography, with compound **15** eluting at 42% ethyl acetate in hexanes as a white solid in 68% yield (342 mg, 1.11 mmol). $^1\text{H NMR}$ (400 MHz, CDCl_3 -*d*): δ 8.21 (s, 1H), 7.86 (s, 1H), 4.59 (s, 2H), 4.02 (s, 3H). ESI-MS(+) calculated for $[\text{C}_8\text{H}_8\text{Br}_2\text{NO}_2]^+$ m/z 307.89, found m/z 308.07 and 310.00 $[\text{M}+\text{H}]^+$.

Methyl 4-bromo-6-((diethoxyphosphoryl)methyl)picolinate (16).

In a round bottom flask, **15** (3.5 g, 11.39 mmol) and triethyl phosphite (5.7 g, 34.16 mmol) were dissolved in toluene (30 mL). The reaction was heated at 140°C for 22 h. Excess triethyl phosphite and toluene were removed in vacuo, and the crude product was purified via flash column chromatography. Compound **16** eluted at 70% ethyl acetate in hexanes as a clear oil in 92% yield (3.9 g, 10.52 mmol). $^1\text{H NMR}$ (400 MHz, CDCl_3 -*d*): δ 8.17 (s, 1H), 7.78 (s, 1H), 4.12 (dq, $J = 10.2, 3.6$ Hz, 4H), 3.99 (s, 3H), 3.50 (d, $J = 22.0$ Hz, 2H), 1.29 (t, $J = 7.0$ Hz, 6H). ESI-MS(+) calculated for $[\text{C}_{12}\text{H}_{18}\text{BrNO}_5\text{P}]^+$ m/z 366.01, found m/z 366.03 $[\text{M}+\text{H}]^+$.

General procedures for the synthesis of compounds 17a – 17m.—In a round bottom flask, compound **16** (1 eq.), the corresponding boronic acid (1.2 eq.) and $\text{K}_3\text{O}_4\text{P}$ (2 eq.) were dissolved in 1,4-dioxanes (5 mL). The solution was purged under N_2 for 20 min, followed by the addition of tetrakis(triphenylphosphine)palladium(0) (0.1 eq.). The reaction was heated to 80°C for 18 h under N_2 . The crude mixture was filtered through a pad of celite, washed with ethyl acetate, and the combined organic layers were concentrated in vacuo. The crude products were purified via flash column chromatography to afford derivatives **17a – 17m**.

Methyl 6-((diethoxyphosphoryl)methyl)-4-phenylpicolinate (17a).

Yield: 74% (59 mg, 0.16 mmol). $^1\text{H NMR}$ (400 MHz, $\text{MeOD}-d_4$): δ 8.26 (s, 1H), 7.90 (d, $J = 2.1$ Hz, 1H), 7.77 (d, $J = 6.5$ Hz, 2H), 7.65 – 7.31 (m, 3H), 4.28 – 4.07 (m, 4H), 3.65 (d, $J = 22.2$ Hz, 2H), 1.28 (t, $J = 7.0$ Hz, 6H). ESI-MS(+) calculated for $[\text{C}_{18}\text{H}_{23}\text{NO}_5\text{P}]^+$ m/z 364.13, found m/z 364.11 $[\text{M}+\text{H}]^+$.

Methyl 6-((diethoxyphosphoryl)methyl)-4-(4-methoxyphenyl)picolinate (17b).

Yield: 79% (120 mg, 0.31 mmol). $^1\text{H NMR}$ (400 MHz, $\text{DMSO}-d_6$): δ 8.14 (s, 1H), 7.87 (s, 1H), 7.79 (d, $J = 7.3$ Hz, 2H), 7.10 (d, $J = 7.7$ Hz, 2H), 4.11 – 3.94 (m, 4H), 3.89 (s, 3H), 3.82 (s, 3H), 3.56 (d, $J = 21.7$ Hz, 2H), 1.18 (t, $J = 6.2$ Hz, 6H). ESI-MS(+) calculated for $[\text{C}_{19}\text{H}_{25}\text{NO}_6\text{P}]^+$ m/z 394.14, found m/z 394.28 $[\text{M}+\text{H}]^+$.

Methyl 6-((diethoxyphosphoryl)methyl)-4-(3-methoxyphenyl)picolinate (17c).

Yield: 58% (86 mg, 0.22 mmol). ¹H NMR (400 MHz, MeOD-*d*₄): δ 8.26 (s, 1H), 7.90 (s, 1H), 7.45 (t, *J* = 8.0 Hz, 1H), 7.34 (d, *J* = 7.8 Hz, 1H), 7.30 (s, 1H), 7.07 (d, *J* = 8.2 Hz, 1H), 4.21 – 4.07 (m, 4H), 4.00 (s, 3H), 3.88 (s, 3H), 3.66 (d, *J* = 22.2 Hz, 2H), 1.29 (t, *J* = 7.0 Hz, 6H). ESI-MS(+) calculated for [C₁₉H₂₅NO₆P]⁺ *m/z* 394.14, found *m/z* 416.13 [M+Na]⁺.

Methyl 6-((diethoxyphosphoryl)methyl)-4-(2-methoxyphenyl)picolinate (17d).

Yield: 87% (125 mg, 0.32 mmol). ¹H NMR (400 MHz, MeOD-*d*₄): δ 8.20 (s, 1H), 7.81 (s, 1H), 7.50 – 7.36 (m, 2H), 7.15 (d, *J* = 8.4 Hz, 1H), 7.09 (t, *J* = 7.5 Hz, 1H), 4.24 – 4.06 (m, 4H), 3.98 (s, 3H), 3.86 (s, 3H), 3.63 (d, *J* = 22.2 Hz, 2H), 1.28 (t, *J* = 7.0 Hz, 6H). ESI-MS(+) calculated for [C₁₉H₂₅NO₆P]⁺ *m/z* 394.14, found *m/z* 416.13 [M+Na]⁺.

Methyl 6-((diethoxyphosphoryl)methyl)-4-(4-hydroxyphenyl)picolinate (17e).

Yield: 20% (27 mg, 0.07 mmol). ¹H NMR (400 MHz, MeOD-*d*₄): δ 8.21 (s, 1H), 7.83 (s, 1H), 7.65 (d, *J* = 6.4 Hz, 2H), 6.92 (d, *J* = 6.7 Hz, 2H), 4.31 – 4.04 (m, 4H), 3.99 (s, 3H), 3.61 (d, *J* = 23.0 Hz, 2H), 1.28 (t, *J* = 7.0 Hz, 7H). ESI-MS(+) calculated for [C₁₈H₂₃NO₆P]⁺ *m/z* 380.12, found *m/z* 402.13 [M+Na]⁺.

Methyl 6-((diethoxyphosphoryl)methyl)-4-(3-hydroxyphenyl)picolinate (17f).

Yield: 90% (135 mg, 0.40 mmol). ¹H NMR (400 MHz, MeOD-*d*₄): δ 8.23 (s, 1H), 7.86 (s, 1H), 7.35 (t, *J* = 7.9 Hz, 1H), 7.22 (d, *J* = 7.9 Hz, 1H), 7.16 (s, 1H), 6.92 (d, *J* = 8.0 Hz, 1H), 4.21 – 4.06 (m, 4H), 4.00 (s, 3H), 3.65 (d, *J* = 20.8 Hz, 2H), 1.29 (t, *J* = 6.3 Hz, 6H). ESI-MS(+) calculated for [C₁₈H₂₃NO₆P]⁺ *m/z* 380.12, found *m/z* 402.13 [M+Na]⁺.

Methyl 6-((diethoxyphosphoryl)methyl)-4-(2-hydroxyphenyl)picolinate (17g).

Yield: 63% (91 mg, 0.24 mmol). ¹H NMR (400 MHz, MeOD-*d*₄): δ 8.31 (s, 1H), 7.91 (s, 1H), 7.41 (d, *J* = 7.4 Hz, 1H), 7.28 (t, *J* = 7.8 Hz, 1H), 7.02 – 6.80 (m, 2H), 4.21 – 4.05 (m, 4H), 3.98 (s, 3H), 3.63 (d, *J* = 22.1 Hz, 2H), 1.28 (t, *J* = 7.0 Hz, 6H). ESI-MS(+) calculated for [C₁₈H₂₃NO₆P]⁺ *m/z* 380.12, found *m/z* 402.13 [M+Na]⁺.

Methyl 4-(4-acetamidophenyl)-6-((diethoxyphosphoryl)methyl)picolinate (17h)

Yield: 43% (72 mg, 0.170 mmol). ¹H NMR (400 MHz, MeOD-*d*₄): δ 8.36 (s, 1H), 8.02 (s, 1H), 7.87 – 7.72 (m, 4H), 4.23 – 4.09 (m, 4H), 4.03 (s, 3H), 3.72 (d, *J* = 22.3 Hz, 2H), 2.16 (s, 3H), 1.29 (t, *J* = 7.0 Hz, 6H). ESI-MS(+) calculated for [C₂₀H₂₆N₂O₆P]⁺ *m/z* 421.15, found *m/z* 421.20 [M+H]⁺.

Methyl 4-(3-acetamidophenyl)-6-((diethoxyphosphoryl)methyl)picolinate (17i).

Yield: 39% (60 mg, 0.14 mmol). ¹H NMR (400 MHz, CDCl₃-*d*): δ 8.22 (s, 1H), 8.16 (s, 1H), 7.85 (d, *J* = 6.8 Hz, 2H), 7.68 (d, *J* = 7.0 Hz, 1H), 7.43 – 7.32 (m, 2H), 4.28 – 4.05 (m, 4H), 4.00 (s, 3H), 3.67 (d, *J* = 21.9 Hz, 2H), 2.22 (s, 3H), 1.30 (t, *J* = 7.1 Hz, 6H). ESI-MS(+) calculated for [C₂₀H₂₆N₂O₆P]⁺ *m/z* 421.15, found *m/z* 421.19 [M+H]⁺.

Methyl 4-(2-acetamidophenyl)-6-((diethoxyphosphoryl)methyl)picolinate (17j).

Yield: 84% (136 mg, 0.32 mmol). $^1\text{H NMR}$ (400 MHz, MeOD- d_4): δ 8.17 (s, 1H), 7.80 (s, 1H), 7.64 – 7.29 (m, 4H), 4.32 – 4.08 (m, 4H), 4.02 (s, 3H), 3.74 (d, J = 22.3 Hz, 2H), 1.99 (s, 3H), 1.31 (t, J = 7.0 Hz, 6H). ESI-MS(+) calculated for $[\text{C}_{20}\text{H}_{26}\text{N}_2\text{O}_6\text{P}]^+$ m/z 421.15, found m/z 421.21 $[\text{M}+\text{H}]^+$.

Methyl 4-(4-chlorophenyl)-6-((diethoxyphosphoryl)methyl)picolinate (17k).

Yield: 60% (91 mg, 0.23 mmol). $^1\text{H NMR}$ (400 MHz, MeOD- d_4): δ 8.28 (s, 1H), 7.91 (s, 1H), 7.80 (d, J = 8.7 Hz, 2H), 7.55 (d, J = 8.6 Hz, 2H), 4.23 – 4.08 (m, 5H), 4.00 (s, 3H), 3.66 (d, J = 22.2 Hz, 2H), 1.28 (t, J = 7.1 Hz, 6H). ESI-MS(+) calculated for $[\text{C}_{18}\text{H}_{22}\text{ClNO}_5\text{P}]^+$ m/z 398.09, found m/z 398.24 $[\text{M}+\text{H}]^+$.

Methyl 4-(3-chlorophenyl)-6-((diethoxyphosphoryl)methyl)picolinate (17l).

Yield: 42% (63 mg, 0.16 mmol). $^1\text{H NMR}$ (400 MHz, MeOD- d_4): δ 8.28 (s, 1H), 7.93 (s, 1H), 7.84 (s, 1H), 7.78 – 7.68 (m, 1H), 7.61 – 7.47 (m, 2H), 4.24 – 4.08 (m, 4H), 4.01 (s, 3H), 3.67 (d, J = 22.0 Hz, 2H), 1.29 (t, J = 6.8 Hz, 6H). ESI-MS(+) calculated for $[\text{C}_{18}\text{H}_{22}\text{ClNO}_5\text{P}]^+$ m/z 398.09, found m/z 398.15 $[\text{M}+\text{H}]^+$.

Methyl 4-(2-chlorophenyl)-6-((diethoxyphosphoryl)methyl)picolinate (17m).

Yield: 71% (114 mg, 0.29 mmol). $^1\text{H NMR}$ (400 MHz, MeOD- d_4): δ 8.11 (s, 1H), 7.74 (s, 1H), 7.61 – 7.40 (m, 4H), 4.23 – 4.07 (m, 4H), 3.99 (s, 3H), 3.67 (d, J = 22.2 Hz, 2H), 1.28 (t, J = 7.1 Hz, 6H). ESI-MS(+) calculated for $[\text{C}_{18}\text{H}_{22}\text{ClNO}_5\text{P}]^+$ m/z 398.09, found m/z 398.13 $[\text{M}+\text{H}]^+$.

General procedures for the synthesis of 18a – 18m.—Compounds **17a – 17m** were dissolved in a solution of 6 M HCl and heated to 100°C for 24 h. Excess HCl was removed in vacuo followed by co-evaporation with copious amounts of water and MeOH until precipitate was observed. The precipitate was collected via vacuum filtration and washed with cold water to afford products **18a – 18m**.

4-Phenyl-6-(phosphonomethyl)picolinic acid (18a).

Yield: 29% (14 mg, 0.05 mmol). $^1\text{H NMR}$ (400 MHz, MeOD- d_4): δ 8.65 (s, 1H), 8.39 (s, 1H), 8.14 – 7.57 (m, 5H), 3.82 (d, J = 22.3 Hz, 2H). ESI-MS(–) calculated for $[\text{C}_{13}\text{H}_{11}\text{NO}_5\text{P}]^-$ m/z 292.03, found m/z 292.04 $[\text{M}-\text{H}]^-$.

4-(4-Methoxyphenyl)-6-(phosphonomethyl)picolinic acid (18b).

Yield: 61% (48 mg, 0.15 mmol). $^1\text{H NMR}$ (400 MHz, DMSO- d_6): δ 8.08 (s, 1H), 7.82 (s, 1H), 7.75 (d, J = 8.6 Hz, 2H), 7.09 (d, J = 8.5 Hz, 2H), 3.81 (s, 3H), 3.30 (d, J = 21.4 Hz, 2H). $^{13}\text{C NMR}$ (126 MHz, DMSO- d_6): δ 166.7, 161.0, 156.2, 148.9, 148.3, 129.2, 128.7, 124.3, 119.6, 115.2, 55.8, 38.3. ESI-MS(–) calculated for $[\text{C}_{14}\text{H}_{13}\text{NO}_6\text{P}]^-$ m/z 322.05, found m/z 322.10 $[\text{M}-\text{H}]^-$.

4-(3-Methoxyphenyl)-6-(phosphonomethyl)picolinic acid (18c).

Yield: 71% (50 mg, 0.15 mmol). ^1H NMR (400 MHz, MeOD- d_4): δ 8.33 (s, 1H), 8.01 (s, 1H), 7.53 – 7.31 (m, 3H), 7.09 (d, J = 7.4 Hz, 1H), 3.89 (s, 3H), 3.56 (d, J = 21.8 Hz, 2H). ^{13}C NMR (126 MHz, DMSO- d_6): δ 166.7, 160.4, 156.2, 149.4, 148.6, 138.8, 131.0, 125.3, 120.4, 119.6, 115.7, 112.7, 55.8, 38.4. ESI-MS(–) calculated for $[\text{C}_{14}\text{H}_{13}\text{NO}_6\text{P}]^-$ m/z 322.05, found m/z 322.02 $[\text{M}-\text{H}]^-$.

4-(2-Methoxyphenyl)-6-(phosphonomethyl)picolinic acid (18d).

Yield: 67% (67 mg, 0.21 mmol). ^1H NMR (400 MHz, MeOD- d_4): δ 8.32 (s, 1H), 7.96 (s, 1H), 7.59 – 7.38 (m, 2H), 7.17 (d, J = 8.2 Hz, 1H), 7.11 (t, J = 7.4 Hz, 1H), 3.88 (s, 3H), 3.55 (d, J = 21.7 Hz, 2H). ^{13}C NMR (126 MHz, DMSO- d_6): δ 166.7, 156.7, 155.5, 147.9, 147.2, 131.2, 130.6, 127.7, 126.6, 123.3, 121.5, 112.5, 56.1, 38.3. ESI-MS(–) calculated for $[\text{C}_{14}\text{H}_{13}\text{NO}_6\text{P}]^-$ m/z 322.05, found m/z 322.04 $[\text{M}-\text{H}]^-$.

4-(4-Hydroxyphenyl)-6-(phosphonomethyl)picolinic acid (18e).

Yield: 82% (16 mg, 0.06 mmol). ^1H NMR (400 MHz, MeOD- d_4): δ 8.38 (s, 1H), 8.08 (s, 1H), 7.81 (d, J = 8.2 Hz, 2H), 6.96 (d, J = 8.0 Hz, 2H), 3.56 (d, J = 21.4 Hz, 2H). ^{13}C NMR (126 MHz, DMSO- d_6): δ 166.7, 159.5, 155.9, 148.8, 148.7, 128.7, 127.5, 124.0, 119.4, 116.6, 38.2. ESI-MS(–) calculated for $[\text{C}_{13}\text{H}_{11}\text{NO}_6\text{P}]^-$ m/z 308.03, found m/z 308.02 $[\text{M}-\text{H}]^-$.

4-(3-Hydroxyphenyl)-6-(phosphonomethyl)picolinic acid (18f).

Yield: 82% (77 mg, 0.30 mmol). ^1H NMR (400 MHz, MeOD- d_4): δ 8.47 (s, 1H), 8.21 (s, 1H), 7.48 – 7.33 (m, 2H), 7.29 (s, 1H), 7.01 (d, J = 7.4 Hz, 1H), 3.73 (d, J = 22.1 Hz, 2H). ^{13}C NMR (126 MHz, DMSO- d_6): δ 166.6, 158.6, 156.2, 148.9, 148.9, 138.5, 131.0, 125.0, 120.2, 118.0, 117.0, 113.9, 38.3. ESI-MS(–) calculated for $[\text{C}_{13}\text{H}_{11}\text{NO}_6\text{P}]^-$ m/z 308.03, found m/z 308.05 $[\text{M}-\text{H}]^-$.

4-(2-Hydroxyphenyl)-6-(phosphonomethyl)picolinic acid (18g).

Yield: 76% (56 mg, 0.18 mmol). ^1H NMR (400 MHz, MeOD- d_4): δ 8.87 (s, 1H), 8.48 (s, 1H), 7.68 (d, J = 6.7 Hz, 1H), 7.45 (t, J = 7.1 Hz, 1H), 7.13 – 7.01 (m, 1H), 3.86 (d, J = 22.4 Hz, 2H). ^{13}C NMR (126 MHz, DMSO- d_6): δ 166.8, 155.5, 155.3, 147.8, 147.6, 130.9, 130.5, 127.2, 124.5, 123.1, 120.2, 116.8, 38.4. ESI-MS(–) calculated for $[\text{C}_{13}\text{H}_{11}\text{NO}_6\text{P}]^-$ m/z 308.03, found m/z 308.09 $[\text{M}-\text{H}]^-$.

4-(4-Aminophenyl)-6-(phosphonomethyl)picolinic acid (18h).

Yield: 56% (14 mg, 0.05 mmol). ^1H NMR (400 MHz, MeOD- d_4): δ 8.68 (s, 1H), 8.43 (s, 1H), 8.14 (d, J = 8.2 Hz, 2H), 7.56 (d, J = 8.2 Hz, 2H), 3.86 (d, J = 22.4 Hz, 2H). ^{13}C NMR (126 MHz, DMSO- d_6): δ 166.6, 155.5, 151.1, 149.2, 148.6, 128.2, 123.1, 123.0, 118.5, 114.6, 38.0. ESI-MS(–) calculated for $[\text{C}_{13}\text{H}_{12}\text{N}_2\text{O}_5\text{P}]^-$ m/z 307.05, found m/z 307.09 $[\text{M}-\text{H}]^-$.

4-(3-Aminophenyl)-6-(phosphonomethyl)picolinic acid (18i).

Yield: 96% (48 mg, 0.16 mmol). ¹H NMR (400 MHz, MeOD-*d*₄): δ 8.35 (s, 1H), 8.01 (s, 1H), 7.96 – 7.47 (m, 4H), 3.59 (d, *J* = 21.9 Hz, 2H). ¹³C NMR (126 MHz, DMSO-*d*₆): δ 166.4, 156.3, 148.9, 148.2, 138.3, 137.9, 131.1, 125.1, 123.6, 122.4, 120.3, 119.4, 38.3. ESI-MS(–) calculated for [C₁₃H₁₂N₂O₅P][–] *m/z* 307.05, found *m/z* 307.09 [M-H][–].

4-(2-Aminophenyl)-6-(phosphonomethyl)picolinic acid (18j).

yield: 60% (60 mg, 0.19 mmol). ¹H NMR (400 MHz, MeOD-*d*₄): δ 8.24 (s, 1H), 7.87 (s, 1H), 7.54 – 7.32 (m, 2H), 7.25 – 7.05 (m, 2H), 3.57 (d, *J* = 21.7 Hz, 2H). ¹³C NMR (126 MHz, DMSO-*d*₆): δ 166.7, 155.8, 155.7, 148.9, 148.7, 145.9, 130.3, 127.2, 122.6, 122.1, 117.3, 116.3, 38.3. ESI-MS(–) calculated for [C₁₃H₁₂N₂O₅P][–] *m/z* 307.05, found *m/z* 307.06 [M-H][–].

4-(4-Chlorophenyl)-6-(phosphonomethyl)picolinic acid (18k).

Yield: 97% (60 mg, 0.18 mmol). ¹H NMR (400 MHz, DMSO-*d*₆): δ 8.13 (s, 1H), 7.86 (s, 2H), 7.83 (d, *J* = 8.1 Hz, 3H), 7.62 (d, *J* = 8.1 Hz, 2H), 3.34 (d, *J* = 21.5 Hz, 2H). ¹³C NMR (126 MHz, DMSO-*d*₆): δ 166.6, 156.3, 149.1, 147.5, 136.0, 135.0, 129.8, 129.2, 125.0, 120.2, 38.3. ESI-MS(–) calculated for [C₁₃H₁₀ClNO₅P][–] *m/z* 326.00, found *m/z* 326.01 [M-H][–].

4-(3-Chlorophenyl)-6-(phosphonomethyl)picolinic acid (18l).

Yield: 90% (47 mg, 0.14 mmol). ¹H NMR (400 MHz, DMSO-*d*₆): δ 8.14 (s, 1H), 7.95 – 7.35 (m, 5H), 3.34 (d, *J* = 21.5 Hz, 2H). ¹³C NMR (126 MHz, DMSO-*d*₆): δ 166.6, 156.4, 149.1, 147.2, 139.4, 134.6, 131.7, 129.8, 127.2, 126.2, 125.2, 120.4, 38.4. ESI-MS(–) calculated for [C₁₃H₁₀ClNO₅P][–] *m/z* 326.00, found *m/z* 325.97 [M-H][–].

4-(2-Chlorophenyl)-6-(phosphonomethyl)picolinic acid (18m).

Yield: 72% (67 mg, 0.20 mmol). ¹H NMR (400 MHz, MeOD-*d*₄) δ 8.57 (s, 1H), 8.30 (s, 1H), 7.77 – 7.48 (m, 4H), 3.89 (d, *J* = 22.5 Hz, 2H). ¹³C NMR (126 MHz, DMSO-*d*₆): δ 166.5, 155.8, 148.2, 147.5, 137.0, 131.7, 131.4, 131.2, 130.7, 128.4, 127.9, 123.2, 38.3. ESI-MS(–) calculated for [C₁₃H₁₀ClNO₅P][–] *m/z* 326.00, found *m/z* 325.98 [M-H][–].

Determination of IC₅₀ values for MBL inhibition

MBL metalloforms NDM-1, IMP-1, and VIM-2 were over-expressed and purified as previously described.²⁸ The IC₅₀ values for which meropenem was used as a substrate is described. The decrease in absorption of meropenem at 300 nm (buffer: 50 mM HEPES, 2mM CHAPS, pH 7) was monitored in UV-transparent 96 well plates (Corning product #3635).⁴⁵ Briefly, 20 μL of each compound at various concentrations (final concentration 0 – 10 μM) was added to each well, followed by addition of 50 μL NDM-1 (final concentration of either 5 or 10 nM). The wells were incubated at 25 °C for 20 min. Next, 30 μL of meropenem (final concentration 180 μM) was added to each well to initiate the reaction. The plate was then centrifuged at 600 rpm for 30 s to eliminate air bubbles, and placed into a Synergy H4 plate reader (BioTek). The absorbance was monitored at 300 nm

over 5 min with 15 s intervals. The Abs_{300nm}/min was calculated from each slope as described below, fixing the uninhibited value at 100%, and solving for both the IC_{50} and Hill coefficient values.²⁸

The IC_{50} values for which Fluorocillin was used as a substrate were determined as described previously,²⁸ with minor modifications made to the volume of reagents used. Briefly, 20 μL of each compound at various concentrations (final concentration 0.001 – 10 μM) was added to each well, followed by addition of 50 μL enzyme (final concentration, NDM-1, 0.2 nM; VIM-2, 2 nM; IMP-1, 0.06 nM). Each plate was incubated for 20 min at 25 °C, followed by the addition of 30 μL Fluorocillin (final concentration 87 nM). The hydrolysis of Fluorocillin is monitored at $\lambda_{ex/em}$ of 495/525 nm. Plates were prepared in parallel to minimize any variability due to compound storage and handling. The rates of fluorescence increase are determined and IC_{50} values determined as described above for the chromogenic assay.

Equilibrium dialysis

ZnN-NDM-1 (final concentration 8 μM) in 5 mL of 100 mM ammonium acetate, pH 7.5, was mixed with the compounds 1 – 4 at concentrations of 0 – 128 μM . After incubation for 1 h, the solutions were dialyzed versus 500 mL of metal-free ammonium acetate, pH 7.5, overnight (dialysis tubing MWCO 6000–8000, Fisherbrand). The Zn(II) content in the resulting NDM-1 samples was determined using inductively coupled plasma with atomic emission spectroscopy (ICP-AES, Perkin Elmer Optima 7300DV). The emission wavelength was set to 213.856 nm, as previously described.²⁸

UV-Visible spectroscopy

To prepare Co(II)-substituted NDM-1, NDM-1 (150 μM) was dialyzed twice against 2 mM EDTA, 50 mM HEPES, pH 6.8, containing 150 mM NaCl, and 2 mM EDTA, followed by three separate dialysis steps against 50 mM HEPES, pH 6.8, containing 150 mM NaCl, and 0.5 g/L Chelex resin. Buffers were exchanged at approximately 12 h intervals. Metal-free NDM-1 was diluted to 300 μM with 50 mM HEPES, pH 6.8, containing 150 mM NaCl, 10% glycerol, and 2 mM TCEP (*tris*(2-carboxyethyl)phosphine). $CoCl_2$ (100 mM stock in water) was added to result in a protein with 2 molar equivalents of Co(II). The resulting CoCo-NDM-1 enzyme was separated into 500 μL aliquots, and captopril, DPA, and compounds 1 – 4 (stock solutions of 50 mM in DMSO) were added to result in samples with 2 molar equivalents of compound. The EDTA stock was dissolved in water. The samples were then incubated on ice for 5 min. The samples were added to a 500 μL quartz cuvette, and UV-vis spectra were collected on a PerkinElmer Lambda 750 UV/vis/NIR spectrometer measuring absorbance between 300 and 800 nm at 25 °C. A blank spectrum of apo-NDM-1 (300 μM) was used to generate difference spectra. All data were normalized at 800 nm.

Supplementary Material

Refer to Web version on PubMed Central for supplementary material.

Acknowledgements

We thank Dr. Yongxuan Su for mass spectrometry sample analysis at The Molecular Mass Spectrometry Facility (MMSF) at UC San Diego. This work was supported by the National Institutes of Health (Grant GM111926), the National Science Foundation (Grant CHE1509285 to M.W.C.), and by the Robert A. Welch Foundation (Grant F-1572 to W.F.). S.M.C. is a cofounder of and has an equity interest in Cleave Biosciences and Forge Therapeutics, companies that may potentially benefit from the research results. S.M.C. also serves on the Scientific Advisory Board for these companies. The terms of this arrangement have been reviewed and approved by the University of California, San Diego in accordance with its conflict of interest policies.

References:

1. Bonomo RA, beta-Lactamases: A Focus on Current Challenges. *Cold Spring Harbor Perspect. Med.* 2017, 7.
2. Fisher JF; Meroueh SO; Mobashery S, Bacterial Resistance to beta-Lactam Antibiotics: Compelling Opportunism, Compelling Opportunity. *Chem. Rev.* 2005, 105, 395–424. [PubMed: 15700950]
3. Bush K; Jacoby GA, Updated Functional Classification of beta-Lactamases. *Antimicrob. Agents Chemother.* 2010, 54, 969–976. [PubMed: 19995920]
4. Naas T; Oueslati S; Bonnin RA; Dabos ML; Zavala A; Dortet L; Retaillieu P; Iorga BI, beta-Lactamase Database (BLDB) - Structure and Function. *J. Enzyme Inhib. Med. Chem.* 2017, 32, 917–919. [PubMed: 28719998]
5. Sabath LD; Abraham EP, Zinc as a Cofactor for Cephalosporinase from *Bacillus cereus* 569. *Biochem. J.* 1966, 98, 11–13.
6. Meini MR; Llarrull LI; Vila AJ, Overcoming Differences: The Catalytic Mechanism of Metallo-beta-Lactamases. *FEBS Lett.* 2015, 589, 3419–3432. [PubMed: 26297824]
7. Mojica MF; Bonomo RA; Fast W, B1-Metallo-beta-Lactamases: Where Do We Stand? *Curr. Drug Targets* 2016, 17, 1029–1050. [PubMed: 26424398]
8. Drawz SM; Bonomo RA, Three Decades of beta-Lactamase Inhibitors. *Clin. Microbiol. Rev.* 2010, 23, 160–201. [PubMed: 20065329]
9. Crowder MW; Spencer J; Vila AJ, Metallo-beta-Lactamases: Novel Weaponry for Antibiotic Resistance in Bacteria. *Acc. Chem. Res.* 2006, 39, 721–728. [PubMed: 17042472]
10. Nordmann P; Naas T; Poirel L, Global Spread of Carbapenemase-producing Enterobacteriaceae. *Emerging Infect. Dis.* 2011, 17, 1791–1798. [PubMed: 22000347]
11. Kang JS; Zhang AL; Faheem M; Zhang CJ; Ai N; Buynak JD; Welsh WJ; Oelschlaeger P, Virtual Screening and Experimental Testing of B1 Metallo-beta-lactamase Inhibitors. *J. Chem. Inf. Model.* 2018, 58, 1902–1914. [PubMed: 30107123]
12. Sun Z; Hu L; Sankaran B; Prasad BVV; Palzkill T, Differential Active Site Requirements for NDM-1 beta-Lactamase Hydrolysis of Carbapenem versus Penicillin and Cephalosporin Antibiotics. *Nat. Commun.* 2018, 9, 4524. [PubMed: 30375382]
13. Zhang H; Hao Q, Crystal Structure of NDM-1 Reveals a Common beta-Lactam Hydrolysis Mechanism. *FASEB J.* 2011, 25, 2574–2582. [PubMed: 21507902]
14. Yong D; Toleman MA; Giske CG; Cho HS; Sundman K; Lee K; Walsh TR, Characterization of a New Metallo-beta-lactamase Gene, bla(NDM-1), and a Novel Erythromycin Esterase gene Carried on a Unique Genetic Structure in *Klebsiella pneumoniae* Sequence Type 14 from India. *Antimicrob. Agents Chemother.* 2009, 53, 5046–5054. [PubMed: 19770275]
15. Zou D; Huang Y; Liu W; Yang Z; Dong D; Huang S; He X; Ao D; Liu N; Wang S; Wang Y; Tong Y; Yuan J; Huang L, Complete Sequences of Two Novel blaNDM-1-Harboring Plasmids from Two *Acinetobacter towneri* Isolates in China Associated with the Acquisition of Tn125. *Sci. Rep.* 2017, 7, 9405. [PubMed: 28839253]
16. Gonzalez LJ; Bahr G; Nakashige TG; Nolan EM; Bonomo RA; Vila AJ, Membrane Anchoring Stabilizes and Favors Secretion of New Delhi Metallo-beta-Lactamase. *Nat. Chem. Biol.* 2016, 12, 516–522. [PubMed: 27182662]
17. King D; Strynadka N, Crystal Structure of New Delhi Metallo-beta-lactamase Reveals Molecular Basis for Antibiotic Resistance. *Protein Sci.* 2011, 20, 1484–1491. [PubMed: 21774017]

18. Walsh TR, Emerging Carbapenemases: a Global Perspective. *Int. J. Antimicrob. Agents* 2010, 36, S8–S14.
19. Nordmann P; Poirel L; Toleman MA; Walsh TR, Does Broad-spectrum beta-Lactam Resistance due to NDM-1 Herald the End of the Antibiotic era for Treatment of Infections Caused by Gram-negative Bacteria? *J. Antimicrob. Chemother.* 2011, 66, 689–692. [PubMed: 21393184]
20. Kumarasamy KK; Toleman MA; Walsh TR; Bagaria J; Butt F; Balakrishnan R; Chaudhary U; Doumith M; Giske CG; Irfan S; Krishnan P; Kumar AV; Maharjan S; Mushtaq S; Noorie T; Paterson DL; Pearson A; Perry C; Pike R; Rao B; Ray U; Sarma JB; Sharma M; Sheridan E; Thirunarayan MA; Turton J; Upadhyay S; Warner M; Welfare W; Livermore DM; Woodford N, Emergence of a New Antibiotic Resistance Mechanism in India, Pakistan, and the UK: a Molecular, Biological, and Epidemiological Study. *Lancet Infect. Dis.* 2010, 10, 597–602. [PubMed: 20705517]
21. Liu L; Feng Y; McNally A; Zong Z, blaNDM-21, a New Variant of blaNDM in an Escherichia Coli Clinical Isolate Carrying blaCTX-M-55 and rmtB. *J. Antimicrob. Chemother.* 2018, 73, 2336–2339. [PubMed: 29912337]
22. Cheng Z; Thomas PW; Ju L; Bergstrom A; Mason K; Clayton D; Miller C; Bethel CR; VanPelt J; Tierney DL; Page RC; Bonomo RA; Fast W; Crowder MW, Evolution of New Delhi Metallo-beta-Lactamase (NDM) in the Clinic: Effects of NDM Mutations on Stability, Zinc Affinity, and Mono-Zinc Activity. *J. Biol. Chem.* 2018, 293, 12606–12618. [PubMed: 29909397]
23. Stewart AC; Bethel CR; VanPelt J; Bergstrom A; Cheng Z; Miller CG; Williams C; Poth R; Morris M; Lahey O; Nix JC; Tierney DL; Page RC; Crowder MW; Bonomo RA; Fast W, Clinical Variants of New Delhi Metallo-beta-Lactamase Are Evolving To Overcome Zinc Scarcity. *ACS Infect. Dis.* 2017, 3, 927–940. [PubMed: 28965402]
24. Bahr G; Vitor-Horen L; Bethel CR; Bonomo RA; Gonzalez LJ; Vila AJ, Clinical Evolution of New Delhi Metallo-beta-Lactamase (NDM) Optimizes Resistance under Zn(II) Deprivation. *Antimicrob. Agents Chemother.* 2018, 62 (1), e01849–01817. [PubMed: 29038264]
25. Linciano P; Cendron L; Gianquinto E; Spyraakis F; Tondi D, Ten Years with New Delhi Metallo-beta-Lactamase-1 (NDM-1): From Structural Insights to Inhibitor Design. *ACS Infect. Dis.* 2018.
26. Ju LC; Cheng Z; Fast W; Bonomo RA; Crowder MW, The Continuing Challenge of Metallo-beta-Lactamase Inhibition: Mechanism Matters. *Trends Pharmacol. Sci.* 2018, 39, 635–647. [PubMed: 29680579]
27. Raczynska JE; Shabalin IG; Minor W; Wlodawer A; Jaskolski M, A Close Look onto Structural Models and Primary Ligands of Metallo-beta-Lactamases. *Drug Resist. Updates* 2018, 40, 1–12.
28. Chen AY; Thomas PW; Stewart AC; Bergstrom A; Cheng ZS; Miller C; Bethel CR; Marshal SH; Credille CV; Riley CL; Page RC; Bonomo RA; Crowder MW; Tierney DL; Fast W; Cohen SM, Dipicolinic Acid Derivatives as Inhibitors of New Delhi Metallo-beta-Lactamase-1. *Med Chem* 2017, 60, 7267–7283.
29. Brem J; Cain R; Cahill S; McDonough MA; Clifton IJ; Jimenez-Castellanos JC; Avison MB; Spencer J; Fishwick CWG; Schofield CJ, Structural Basis of Metallo-beta-Lactamase, Serine-beta-Lactamase and Penicillin-binding Protein Inhibition by Cyclic Boronates. *Nat. Commun.* 2016, 7.
30. Albu SA; Koteva K; King AM; Al-Karmi S; Wright GD; Capretta A, Total Synthesis of Aspergillomarasmine A and Related Compounds: A Sulfamidate Approach Enables Exploration of Structure-Activity Relationships. *Angew. Chem. Int. Ed. Engl.* 2016, 55, 13259–13262. [PubMed: 27633338]
31. Liao D; Yang S; Wang J; Zhang J; Hong B; Wu F; Lei X, Total Synthesis and Structural Reassignment of Aspergillomarasmine A. *Angew. Chem. Int. Ed. Engl.* 2016, 55, 4291–4295. [PubMed: 26592805]
32. Koteva K; King AM; Capretta A; Wright GD, Total Synthesis and Activity of the Metallo-beta-lactamase Inhibitor Aspergillomarasmine A. *Angew. Chem. Int. Ed. Engl.* 2016, 55 (6), 2210–2212. [PubMed: 26709849]
33. Cain R; Brem J; Zollman D; McDonough MA; Johnson RM; Spencer J; Makena A; Abboud MI; Cahill S; Lee SY; McHugh PJ; Schofield CJ; Fishwick CWG, In Silico Fragment-Based Design Identifies Subfamily B1 Metallo-beta-lactamase Inhibitors. *Med Chem* 2018, 61 (3), 1255–1260.

34. Chiou J; Wan S; Chan KF; So PK; He D; Chan EW; Chan TH; Wong KY; Tao J; Chen S, Ebselen as a Potent Covalent Inhibitor of New Delhi Metallo-beta-lactamase (NDM-1). *Chem. Commun.* 2015, 51, 9543–9546.
35. Everett M; Sprynski N; Coelho A; Castandet J; Bayet M; Bougnon J; Lozano C; Davies DT; Leiris S; Zalacain M; Morrissey I; Magnet S; Holden K; Warn P; De Luca F; Docquier JD; Lemonnier M, Discovery of a Novel Metallo-beta-Lactamase Inhibitor That Potentiates Meropenem Activity against Carbapenem-Resistant Enterobacteriaceae. *Antimicrob. Agents Chemother.* 2018, 62, e00074–00018. [PubMed: 29530861]
36. Zhang YL; Yang KW; Zhou YJ; LaCuran AE; Oelschlaeger P; Crowder MW, Diaryl-substituted Azolylthioacetamides: Inhibitor Discovery of New Delhi Metallo-beta-Lactamase-1 (NDM-1). *Chemmedchem* 2014, 9, 2445–2448. [PubMed: 25048031]
37. Kalgutkar AS; Scott Daniels J, Chapter 3 Carboxylic Acids and Their Bioisosteres In *Metabolism, Pharmacokinetics and Toxicity of Functional Groups: Impact of Chemical Building Blocks on ADMET*, The Royal Society of Chemistry: 2010; pp 99–167.
38. Ballatore C; Hury DM; Smith AB, Carboxylic Acid (Bio)Isosteres in Drug Design. *Chemmedchem* 2013, 8, 385–395. [PubMed: 23361977]
39. Lassalas P; Gay B; Lasfargeas C; James MJ; Tran V; Vijayendran KG; Brunden KR; Kozlowski MC; Thomas CJ; Smith AB 3rd; Hury DM; Ballatore C, Structure Property Relationships of Carboxylic Acid Isosteres. *Med Chem* 2016, 59, 3183–3203.
40. Chen AY; Adamek RN; Dick BL; Credille CV; Morrison CN; Cohen SM, Targeting Metalloenzymes for Therapeutic Intervention. *Chem. Rev.* 2018, 119, 1323–1455. [PubMed: 30192523]
41. Adamek RN; Credille CV; Dick BL; Cohen SM, Isosteres of Hydroxypyridinethione as Drug-like Pharmacophores for Metalloenzyme Inhibition. *J. Biol. Inorg. Chem.* 2018, 23, 1129–1138. [PubMed: 30003339]
42. Dick BL; Cohen SM, Metal-Binding Isosteres as New Scaffolds for Metalloenzyme Inhibitors. *Inorg. Chem.* 2018, 57, 9538–9543. [PubMed: 30009599]
43. Klingler FM; Wichelhaus TA; Frank D; Cuesta-Bernal J; El-Delik J; Muller HF; Sjuts H; Gottig S; Koenigs A; Pos KM; Pogoryelov D; Proschak E, Approved Drugs Containing Thiols as Inhibitors of Metallo-beta-lactamases: Strategy To Combat Multidrug-Resistant Bacteria. *Med Chem* 2015, 58, 3626–3630.
44. Bergstrom A; Katko A; Adkins Z; Hill J; Cheng Z; Burnett M; Yang H; Aitha M; Mehaffey MR; Brodbelt JS; Tehrani K; Martin NI; Bonomo RA; Page RC; Tierney DL; Fast W; Wright GD; Crowder MW, Probing the Interaction of Aspergillomarasmine A with Metallo-beta-lactamases NDM-1, VIM-2, and IMP-7. *ACS Infect. Dis.* 2018, 4, 135–145. [PubMed: 29091730]
45. Thomas PW; Zheng M; Wu S; Guo H; Liu D; Xu D; Fast W, Characterization of Purified New Delhi Metallo-beta-Lactamase-1. *Biochemistry* 2011, 50, 10102–10113. [PubMed: 22029287]
46. Brem J; van Berkel SS; Zollman D; Lee SY; Gileadi O; McHugh PJ; Walsh TR; McDonough MA; Schofield CJ, Structural Basis of Metallo-beta-Lactamase Inhibition by Captopril Stereoisomers. *Antimicrob. Agents. Chemother.* 2016, 60, 142–150. [PubMed: 26482303]
47. Yang H; Aitha M; Marts AR; Hetrick A; Bennett B; Crowder MW; Tierney DL, Spectroscopic and Mechanistic Studies of Heterodimetallic Forms of Metallo-beta-Lactamase NDM-1. *J. Am. Chem. Soc.* 2014, 136, 7273–7285. [PubMed: 24754678]
48. King DT; Worrall LJ; Gruninger R; Strynadka NC, New Delhi Metallo-beta-lactamase: Structural Insights into beta-Lactam Recognition and Inhibition. *J. Am. Chem. Soc.* 2012, 134, 11362–11365. [PubMed: 22713171]
49. Hinchliffe P; Tanner CA; Krismanich AP; Labbe G; Goodfellow VJ; Marrone L; Desoky AY; Calvopina K; Whittle EE; Zeng F; Avison MB; Bols NC; Siemann S; Spencer J; Dmitrienko GI, Structural and Kinetic Studies of the Potent Inhibition of Metallo-beta-Lactamases by 6-Phosphonomethylpyridine-2-carboxylates. *Biochemistry* 2018, 57, 1880–1892. [PubMed: 29485857]
50. Cheng Y; Prusoff WH, Relationship Between the Inhibition Constant (K₁) and the Concentration of Inhibitor Which Causes 50 per cent Inhibition (I₅₀) of an Enzymatic Reaction. *Biochem. Pharmacol.* 1973, 22, 3099–3108. [PubMed: 4202581]

51. Yamaguchi Y; Ding S; Murakami E; Imamura K; Fuchigami S; Hashiguchi R; Yutani K; Mori H; Suzuki S; Arakawa Y; Kurosaki H, A Demetallation Method for IMP-1 Metallo-beta-Lactamase with Restored Enzymatic Activity Upon Addition of Metal Ion(s). *Chembiochem* 2011, 12, 1979–1983. [PubMed: 21739563]
52. Yamaguchi Y; Kuroki T; Yasuzawa H; Higashi T; Jin W; Kawanami A; Yamagata Y; Arakawa Y; Goto M; Kurosaki H, Probing the Role of Asp-120(81) of Metallo-beta-Lactamase (IMP-1) by Site-directed Mutagenesis, Kinetic Studies, and X-ray Crystallography. *J. Biol. Chem.* 2005, 280, 20824–20832. [PubMed: 15788415]

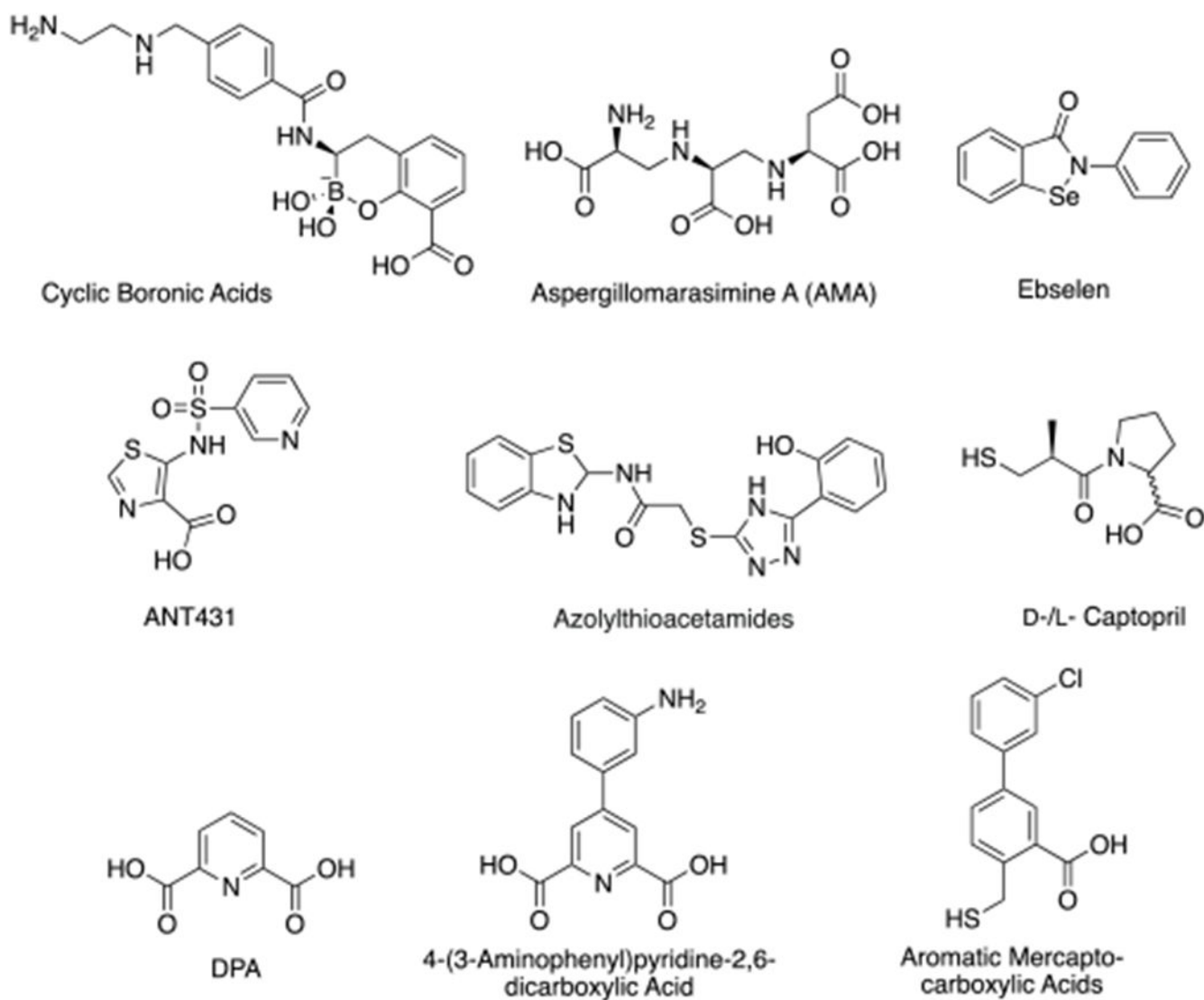


Figure 1.
Representative inhibitors of NDM-1.²⁸⁻³⁶

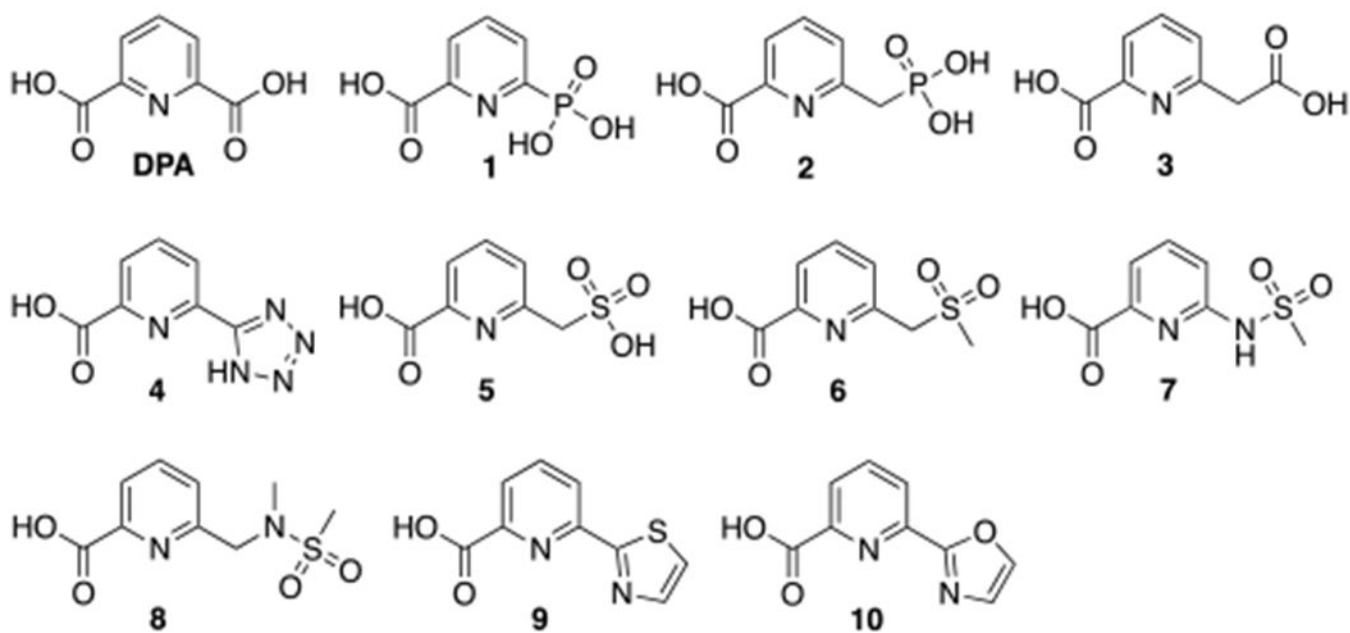


Figure 2.
DPA isosteres reported here.

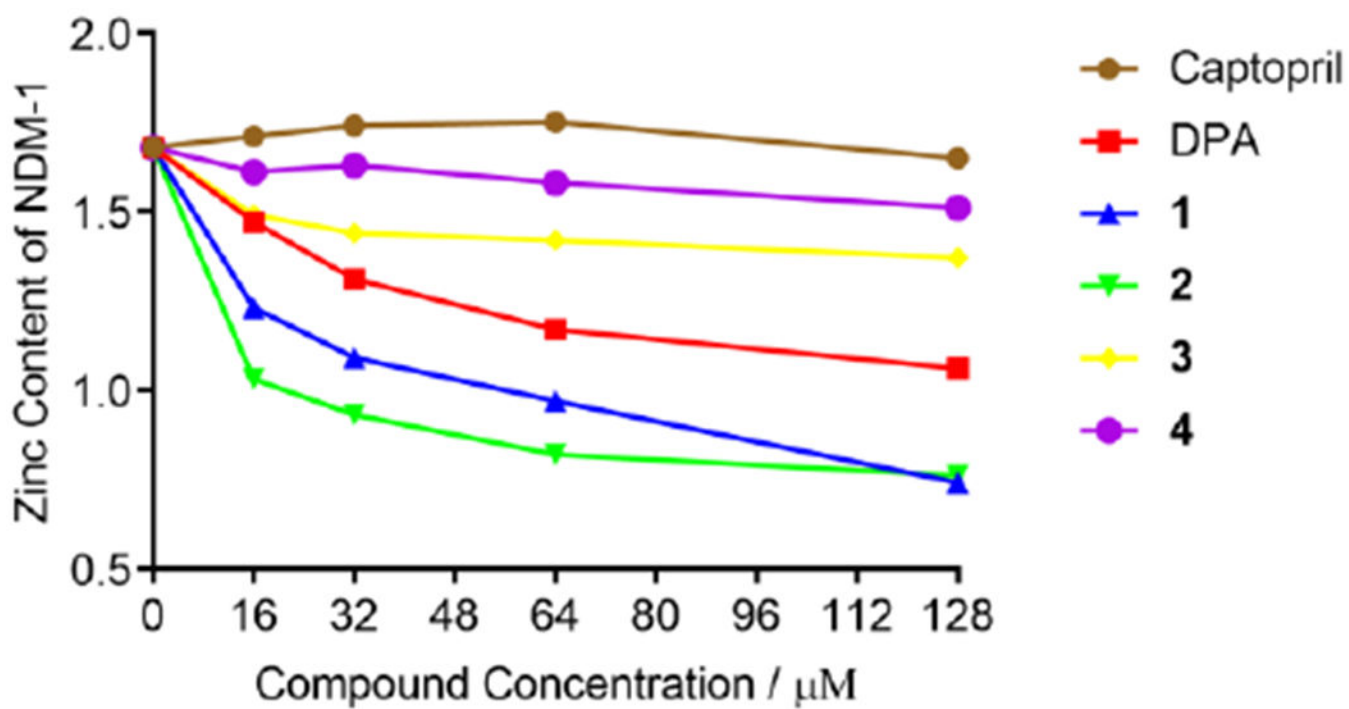


Figure 3. Zn(II) content of NDM-1 (8 μM) upon incubation with increasing concentrations of captopril, DPA, and 1 – 4 (16 μM – 128 μM).

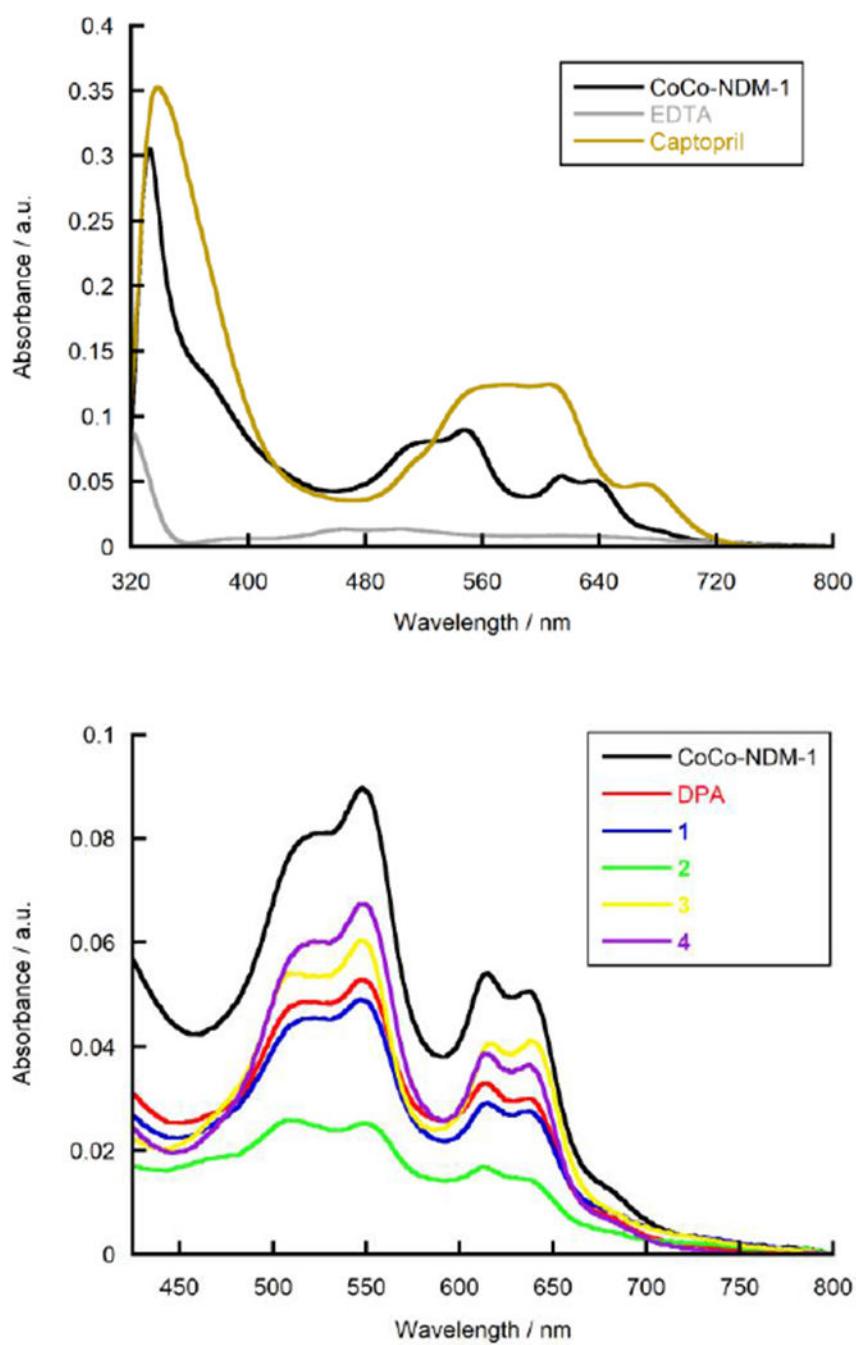


Figure 4. UV-Vis spectrum of CoCo-NDM-1 with captopril and EDTA (*top*), and with **DPA** and **1 – 4** (*bottom*).

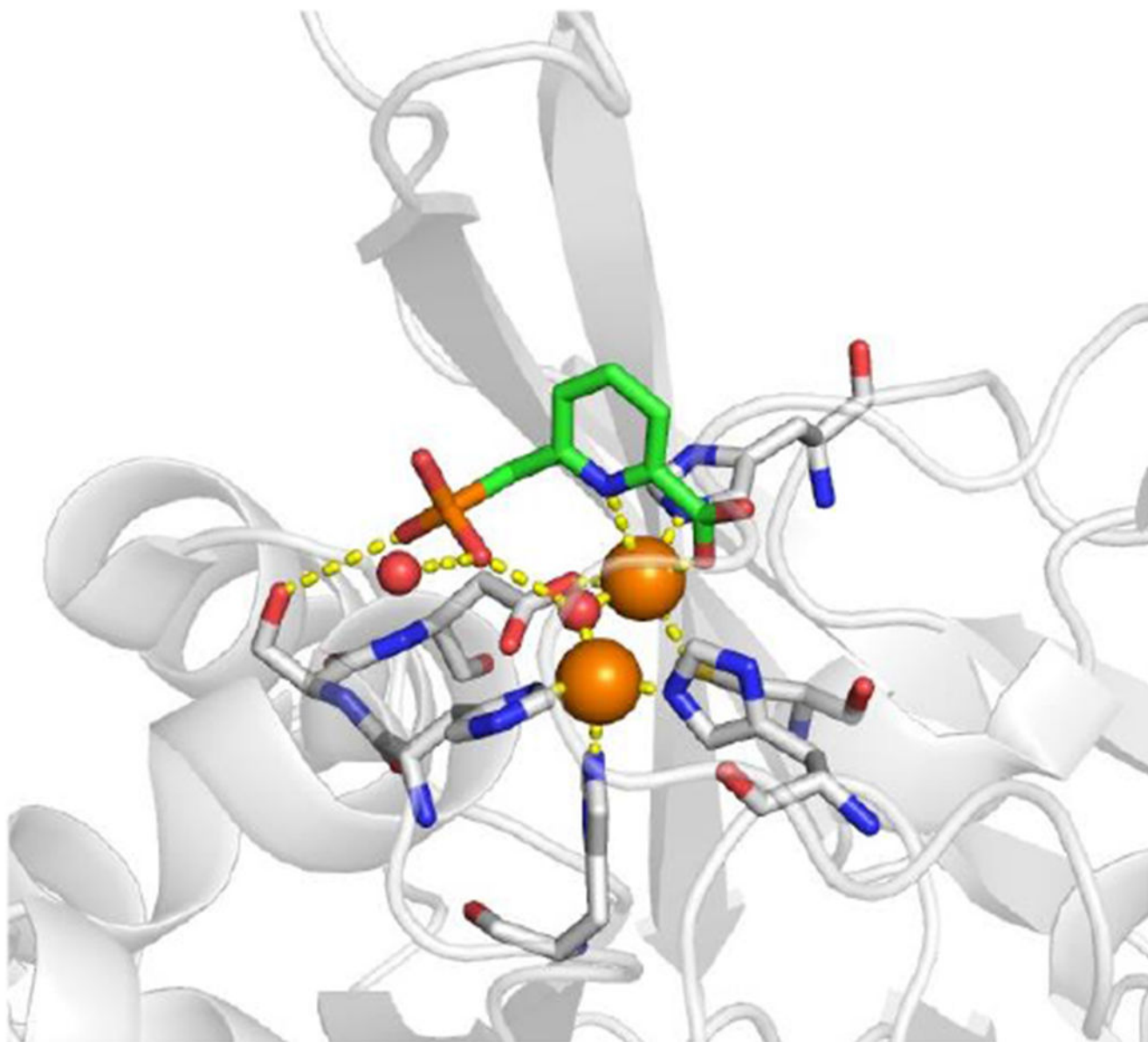
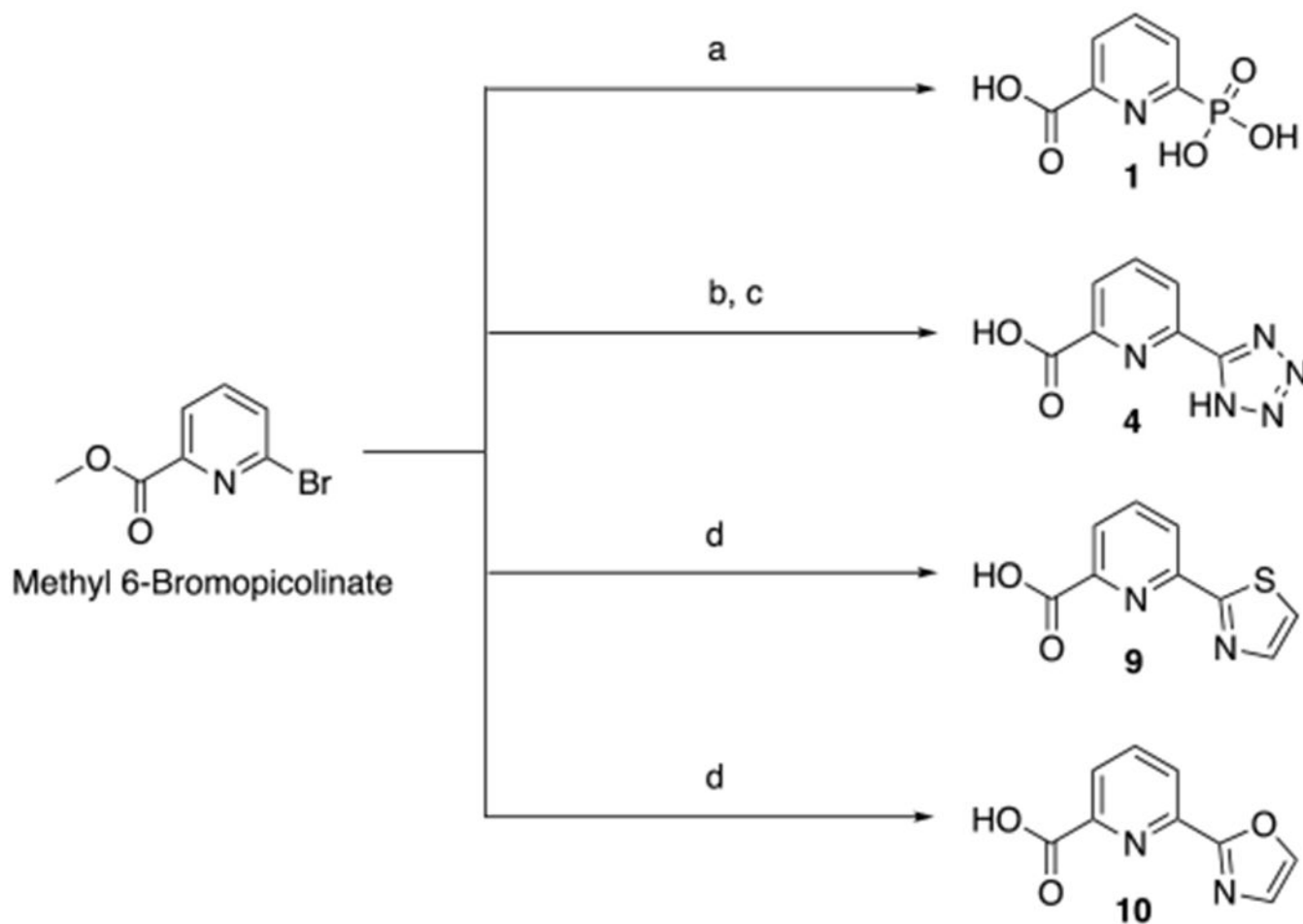
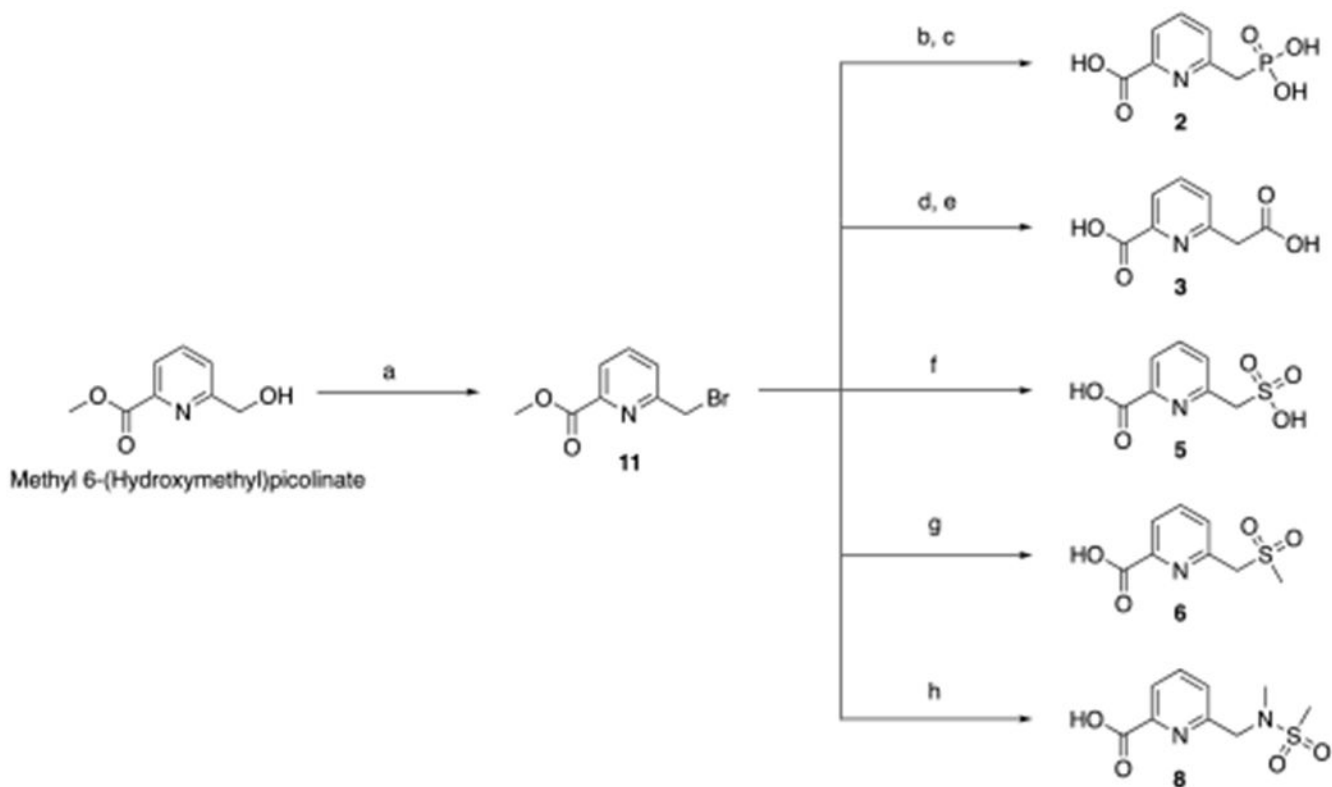


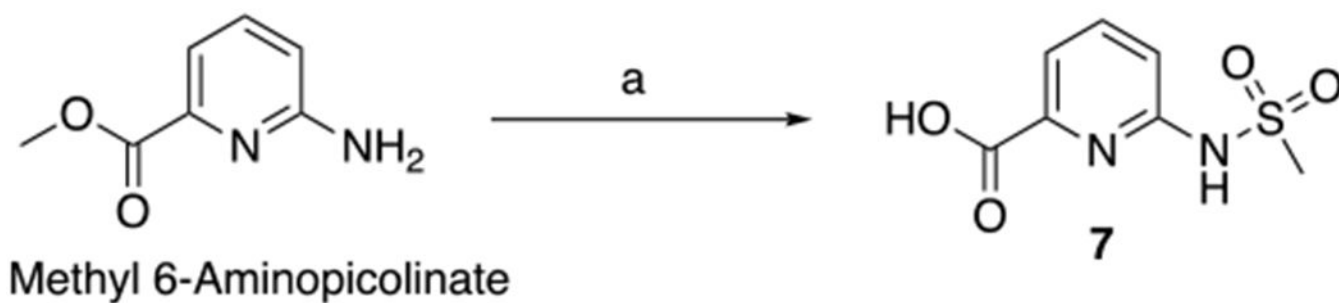
Figure 5. 6-(Phosphonomethyl)picolinic acid (**2**) was reported as a potent inhibitor of B1 and B3 MBLs, and able to restore β -lactam activity in MIC assays. Shown above is **2** complexed with IMP-1 (PDB 5HH4).⁴⁹ Zn(II) ions are shown in orange, coordinating ligands and protein ribbon are shown in grey, **2** is shown in green, and ligand-protein interactions are shown with a yellow-dashed line. Figure was rendered with Molecular Operating Environment (MOE).

**Scheme 1.**

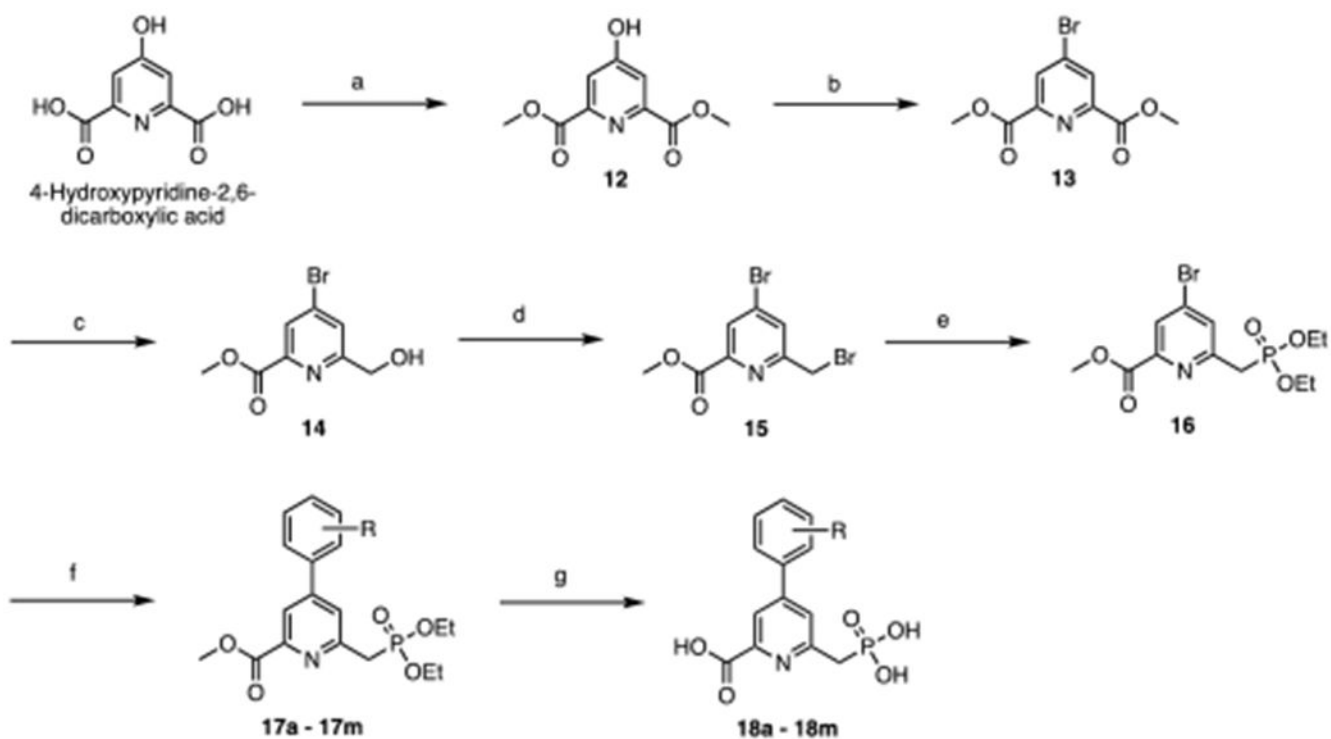
Synthesis of isosteres **1**, **4**, **9**, and **10**. Reagents and conditions: (a) $\text{Pd}_2(\text{dba})_3$, $\text{Pd}(\text{dppf})\text{Cl}_2$, diethylphosphate, triethylamine, toluene, 90°C , 20 h; then 6 M HCl, 100°C , 20 h; *two steps* 19%; (b) CuCN, pyridine, 116°C , 4 h, 21%; (c) NaN_3 , NH_4Cl , DMF, 130°C , 20 h; then 2 M HCl, 25°C , 1 h; *two steps* 98%; (d) 2-(tributylstannyl)thiazole/ 2-(tributylstannyl)oxazole, $\text{Pd}(\text{PPh}_3)_2\text{Cl}_2$, THF, 75°C , 18 h; then 3:1 1 M NaOH:THF, 70°C , 3 h; *two steps* 8-74%.

**Scheme 2.**

Synthesis of isosteres **2**, **3**, **5**, **6**, and **8**. Reagents and conditions: (a) PBr_3 , CHCl_3 , 0°C , 3 h, 70%; (b) $\text{P}(\text{OEt})_3$, toluene, 140°C , 2 h, 80%; (c) 6 M HCl , 100°C , 27 h, 98%; (d) KCN , THF, 50°C , 19 h, 49%; (e) 12 M HCl , 100°C , 12 h, then 1 M NaOH , 60°C , 6 h, 30%; (f) Na_2SO_3 , H_2O , then 4 M HCl , 100°C , 16 h; *two steps* 41%; (g) NaSO_2CH_3 , DMF, 120°C , 2 h, then 3:1 1M NaOH :THF, 70°C , 3 h; *two steps* 43%; (h) $\text{CH}_3\text{NHSO}_2\text{CH}_3$, K_2CO_3 , ACN, 75°C , 25 h; then 1 M NaOH , 70°C , 3 h; *two steps* 55%.

**Scheme 3.**

Synthesis of isostere **7**. Reagents and conditions: (a) Methanesulfonyl chloride, triethylamine, CH₂Cl₂, 0°C, 16 h; then 1 M NaOH: THF, r.t., 16 h; *two steps* 12.4%.

**Scheme 4.**

Synthesis of derivatives of isostere **2** (compounds **18a – 18m**). Reagents and conditions: (a) MeOH, H₂SO₄ (cat.), 70°C, overnight, 60%; (b) P₂O₅, TBAB, toluene, 100°C, 3 h, 75%; (c) NaBH₄, MeOH/CH₂Cl₂, 0°C, 1 h, 80%; (d) PBr₃, CHCl₃, 0°C, 1 h, 68%; (e) P(OEt)₃, toluene, 140°C, 22 h, 92%; (f) boronic acid, K₃O₄P, Pd(PPh₃)₄, 1,4-dioxanes, 80°C, 18 h, 20 – 90%; (g) 6 M HCl, 100 °C, 24 h, 29 – 97%.

Table 1.IC₅₀ values (μM) for **DPA** isostere inhibition of NDM-1 catalyzed meropenem hydrolysis.^[a]

Compound	IC ₅₀	Compound	IC ₅₀
DPA	0.84±0.04	6	>10
1	0.31±0.01	7	>10
2	0.13±0.01	8	>10
3	7.7±0.6	9	>10
4	7.0±0.5	10	>10
5	>10		

[a] Activity measurements were taken in triplicate using varying inhibitor concentrations that bracket each IC₅₀ value, with fitting errors listed above.

Table 2.

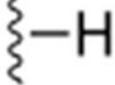
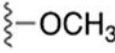
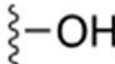
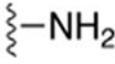
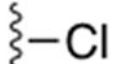
IC₅₀ values (μM) for isostere inhibition of B1 MBL catalyzed Fluorocillin hydrolysis.^[a]

Compound	NDM-1	IMP-1	VIM-2
DPA	0.33±0.04	2.54±0.04	2.34±0.04
1	0.064±0.001	0.85±0.06	0.85±0.02
2	0.068±0.002	0.63±0.01	0.62±0.01
3	2.05±0.09	59±5	35±1
4	2.19±0.13	22±1	27±2

^[a]Activity measurements were taken in triplicate using varying inhibitor concentrations that bracket each IC₅₀ value, with fitting errors listed above.

Table 3.

IC₅₀ values (μM) for compounds **18a** – **18m** against NDM-1 catalyzed meropenem hydrolysis. R refers to substituent in Scheme 4.^[a]

R =		<i>para</i> -	<i>meta</i> -	<i>ortho</i> -		
	18a	0.41±0.02	–	–		
	18b	0.20±0.01	18c	0.42±0.02	18d	0.30±0.01
	18e	0.48±0.01	18f	0.28±0.01	18g	0.28±0.01
	18h	0.30±0.01	18i	0.40±0.02	18j	0.24±0.01
	18k	0.40±0.01	18l	1.29±0.07	18m	0.95±0.05

^[a]Activity measurements were taken in triplicate using varying inhibitor concentrations that bracket each IC₅₀ value, with fitting errors listed above.